POWER-LAW FLUID PRESSURE BEHAVIOUR IN HOMOGENOUS AND NATURALLY FRACTURED RESERVOIR WITH SPHERICAL FLOW

A THESIS

SUBMITTED TO THE DEPARTMENT OF PETROLEUM ENGINEERING OF

AFRICAN UNIVERSITY OF SCIENCE AND TECHNOLOGY

IN PARTIAL FULFILLMENT OF THE REQUIREMENTS

FOR THE DEGREE OF MASTER OF SCIENCE

BY

IWAYEMI, WALE OLANORIN

ABUJA, NIGERIA

APRIL 2013

POWER-LAW FLUID PRESSURE BEHAVIOUR IN HOMOGENOUS AND NATURALLY FRACTURED RESERVOIR WITH SPHERICAL FLOW

By

Iwayemi, Wale Olanorin

RECOMMENDED BY: **…….**

Committee Chair**:** **Dr. Alpheus Igbokoyi**

…..……

Committee Member**:** **Prof. Djebbar Tiab**

…….

Committee Member**:** **Prof. David O. Ogbe**

APPROVED BY: **…….....**

Prof. Godwin Chukwu

Chair, Department of Petroleum Engineering, AUST

…….....

Academic Provost, AUST Abuja

…….

Date

Dedication

I dedicate this work to God Almighty, He who began *"a good work in my life and performed it until its success";* for I was doubtful of success at the onset of this study, but He replaced my doubt with faith.

"Brethren, I count not myself to have apprehended: but this one thing I do, forgetting those things which are behind, and reaching forth unto those things which are before…"

- Apostle Paul, The Holy Bible, *Philippians 3:13*

Acknowledgement

I am deeply grateful to my Supervisor, Dr. Alpheus Igbokoyi – an uncommon man whose quick response, timely supervision and commitment, all through the course of this work, are qualities rare among men.

I would like to thank my committee members – Prof. D. Tiab and Prof. D. Ogbe, for squeezing out time from their tight schedule to validate the authenticity of this work.

I also want to express my appreciation to all my friends and colleagues in the Petroleum Engineering Stream; you made my stay in AUST fun and memorable. I will miss you all. I specially want to thank - Eustace of the Computer Science Stream, for helping me through some of the "mazes" of this work's Matlab code; likewise Ezulike Obinna for his assistance also in this area of my masters' thesis.

My sincere love and appreciation goes to all my families – the Olanorins, Akingoroyes, Shokunbis, Ojajunis and the Oyeleses, for their prayer and support has made this work possible.

This piece will not be complete without mentioning my God given "burden-divider", "joy-multiplier", motivator, the one who shows so much love, care and concern that I often forgot we're not related by blood, my fiancée – Ikeoluwapo Mojolaoluwa Oyelese, you have been a blessing to me, thank you and God bless you bountifully.

Table of Contents

Abstract

Studies have revealed most wells are usually completed with limited or restricted-entry and it's often characterized with spherical flow behaviour. High viscosity crude by their nature may also exhibit Non-Newtonian flow behavior. Fall-off test in polymer injection well with partial completion may also exhibit spherical flow. This paper therefore presents pressure transient analysis for spherical flow behaviour of non-Newtonian power-law fluids in Homogenous and Naturally Fractured Reservoir. In this work, skin and wellbore storage effect are incorporated into the Laplacian space analytical solution derived by Liu Ci-qun (1987).

New pressure and pressure derivative type curves are developed for different flow behaviour index of power-law fluid in Homogenous and Naturally Fractured Reservoirs.

The log-log plot of pressure derivative for the Homogenous system gives a slope of -0.5 at the spherical flow straight line, as expected for Newtonian fluid flow in porous medium; while the slope of non-Newtonian fluid at the spherical flow regime is a function of its flow behaviour index. The pressure derivative plot for Naturally Fractured Reservoir system shows the usual three (3) flow regimes typical of double porosity reservoir system.

This work further develop equations to estimate reservoir, wellbore and power-law flow parameters using Type curve matching and Tiab's Direct Synthesis technique (TDS) --- which uses analytical solution of long-time approximation in evaluating well test data from the log-log plot of pressure and pressure derivative. Equations are developed for both the Homogeneous and Naturally Fractured Reservoir.

List of Figures

List of Tables

Chapter 1

General

1.1 Introduction

The need for improve Oil Recovery and Pressure maintenance of reservoir operating under its natural drive mechanism has brought about Secondary/Enhanced Oil Recovery operations – one of which is Polymer flooding.

Polymer flooding as the name implies is the injection of non-Newtonian fluid, most especially power-law fluids, into the reservoir to sweep/displace oil into the wellbore. Over the years, this method of Oil Recovery has been used and proven to improve recoverable oil; however, field works and studies have also revealed some of its major setbacks. Harvey (1970) stated that a major setback to wider use of polymer flooding seems to be the lack of satisfactory method for predicting the performance of the oil recovery process, and that the basis for much of the difficulty in predicting the performance of Polymer flooding is the lack of clear understanding of the behaviour of high molecular weight polymer fluid injected into the reservoir. Huh and Snow (1985) stated that the distribution of polymer solution within the reservoir is not uniform and, in many cases, is not known and that the fluid viscosity which is dependent on the shear rate at any location in the reservoir are some of the complications involved in Polymer fluid injection. Thus thorough study of non-Newtonian power-law fluid behaviour at reservoir conditions is needed.

Non-Newtonian power-law fluids are fluids whose shear stress and shear rate relationship exhibits non-linear behaviour. Power-law fluids are of two types, Pseudo-plastic and Dilatant fluid. Pseudo-plastic fluid is that which exhibits a decreasing viscosity when higher rates of shear is applied; its flow behaviour index is less than one ($n<1$). Dilatant fluid is that which exhibits increasing viscosity with increasing shear rate; its flow behaviour index is greater than one ($n>1$). Therefore, the unique rheology exhibited by Pseudo-plastic power-law fluid makes it a preferable oil displacement agent used in Polymer flooding operations.

Much work has been reported in Petroleum literature on Pressure transient analysis of power-law fluids in porous media; nonetheless, unsatisfactory Well-test result is not uncommon in field practices. This is often due to most Specialists' strict adherence to examining Well-test data only with techniques developed on the assumption that fluid flows towards the wellbore in horizontal cylindrical-radial pattern, with little or no consideration for spherical flow pattern of fluid toward the wellbore which is often the case in limited /restricted-entry perforation. Limited or restricted-entry problem is usually characterized by spherical flow pattern of fluid into the wellbore especially for thick reservoir; and most of the time, wellbores are completed with small completion interval open to flow so as to prevent or delay the break-through of unwanted fluids into the wellbore. At times, wellbores are partially completed. Sonatrach and

Tiab (2008) noted that in the drilling of Naturally Fractured formation, high mud losses which occur when well encounters fracture zones usually prevent well's total penetration of the reservoir formation thickness; hence penetration in Naturally Fractured Reservoir is rarely total.

Therefore, the problems posed in literatures and Field practices on Well test data analysis suggest a need for attention to be given to spherical flow pattern of fluid in porous media; thus this work, present power-law fluid pressure transient behaviour in Homogenous and Naturally Fractured Reservoir with spherical flow.

1.2 Literature Review

Over the years in the Petroleum literature, abundant number of works has been done both on Newtonian and non-Newtonian fluid flow in porous media. Although the Newtonian fluids has taken a larger share of the studies for the last four decades, much interest has arisen in recent times for non-Newtonian fluids flow in porous media due to the discovery of its advantageous property over Newtonian fluids especially in Secondary recovery operations/Enhanced oil Recovery processes.

Poollen and Jargon (1969) presented equations for steady-state linear and radial flow of non-Newtonian power law fluids through porous media, transient behaviour results, from a finite difference model of a radial system and transient behaviour results from a field test were studied; and the equations presented were solved numerically. He established that the injectivity index increases with rate for a power-law fluid, whereas, for a Newtonian fluid it will remain constant or decrease slightly.

Herbert Harvey and Menzie (1970) presented a method to describe the analysis of rate-dependent effects in the flow of polymer solutions through unconsolidated porous media. Distinctive flow characteristics were noted for several of the solutions that were investigated and possible causes for departure from normal non-Newtonian flow were suggested. He recommended that to adequately characterize the rate-dependent effects which may occur in the vicinity of injection wells in polymer flooding, further study should be done.

Raghavan and Clark (1975) examined the applicability of the spherical flow equations to a well producing from a limited section of a thick anisotropic formation by examining the general characteristic of the dimensionless pressure-time data that describe this type of flow behaviour. From their examination, they deduced that the dimensionless pressure and dimensionless time graph can provide useful information regarding the effect of the producing and shut-in times required to apply the spherical flow equations.

Ershaghi et al. (1976) developed a method for the estimation of an average spherical permeability and static reservoir pressure in a naturally fractured reservoir with spherical flow. He also discussed the procedure for estimating the total fluid capacitance and the fraction of which being contributed by the fracture network. This study employed a reservoir model similar to the double-porosity system described by Warren and Root (1963).

Ikoku and Ramey Jr. (1978) presented solutions of the non-linear partial differential equation of non-Newtonian power law fluids in porous media using the Douglas-Jones predictor-corrector method for numerical solution of non-linear partial differential equations; graphs of dimensionless pressure versus dimensionless radius were also presented. They further presented the analytical solution of transient flow behaviour of non-Newtonian fluids in petroleum reservoir (1979). A new partial differential equation which describes the flow of slightly compressible, non-Newtonian power-law fluid with radial flow in homogenous porous media was derived. Their study introduces new method of well-test analysis for non-Newtonian fluids.

Odeh and Yang (1979) presented similar partial differential equation as Ikoku et al., that describes the flow of non-Newtonian power-law, slightly compressible fluids in porous media, and an approximate solution in closed form was developed for the unsteady-state flow behaviour. They established the theoretical fundamentals of the flow of non-Newtonian power-law fluids in porous media and their analysis of field data indicated that the shear-rate/viscosity relationship determined by viscometers under steady state condition may not be the governing relationship for unsteady state flow condition in porous media; however, the relationship obtained from the analysis gives the integrated average for various permeability and porosity value.

Kohlhass and Abbott (1982) presented techniques for the application of linear and spherical flow analysis to field problems with case history illustrating the techniques, and the types of information that cannot be obtained from the conventional method of analysis were reported.

Okpobiri and Ikoku (1983) investigated pressure fall-off testing in non-Newtonian/Newtonian fluid in composite reservoirs. This study uses a two-phase numerical finite difference model to study the effect of saturation gradients on composite system pressure fall-off tests by accounting for the relative permeability characteristics of the porous medium.

C. Huh and Snow (1985) presented a well testing method which accounts for both the polymer concentration distribution and non-Newtonian fluid rheology. This study assumed radial distribution of polymer fluid within the reservoir.

Vongvuthipornchai et al. (1987) examined pressure fall-off behaviour dominated by wellbore storage and skin subsequent to injection of a non-Newtonian power-law fluid. They further examined the use of the pressure derivative plot technique and its advantages in analyzing pressure fall-off test data. They noted that, due to the non-linear nature of injecting power-law fluid into a formation, fall-off pressure

responses are different from injection pressure responses; thus solutions for injection test case may not be use for fall-off test data analysis.

Liu Ci-qun (1988) studied the transient spherical flow behaviour of a slightly compressible, non-Newtonian power-law fluids flow in porous media and developed a non-linear partial differential equation of this model. He went further to obtain the analytical, asymptotic and approximate solutions by using the methods of Laplace transform and weighted mass conservation. He suggested the solutions obtained from this study may be applied to the theory of one-dimensional spherical flow of non-Newtonian power-law fluid through porous media.

Olanrewaju (1992) studied on the behaviour of non-Newtonian fluids in homogenous reservoirs and further extended the study to non-Newtonian fluid flow in naturally fractured reservoir considering horizontal radial flow pattern in both. Type curves solutions were developed for both homogenous and double porosity reservoir in terms of pressure and pressure derivatives curves originally developed by Bourdet et al. (1989). Some of the results presented in this study show that lower pressure drop or pressure increase will be experienced in a reservoir with a non-Newtonian fluid flowing through its porous medium than for Newtonian fluid flowing through the same system. He suggested that since conventional semi-log straight lines are not present in non-Newtonian fluid flow, semi-log analysis method cannot be use for its well test data.

Bui et al. (2000) presented an analytical solution that describes transient pressure behaviour of partially penetrating wells in naturally fractured reservoir. The solution was obtained by combining the Warren and Root (1963) pseudo-steady state model for NFR with Yildiz and Bassiouni (1990) partially-penetrating well model in homogenous reservoir. Radial flow of fluid within the formation was assumed.

Sonatrach et al. (2006) proposed a method for identifying, on the pressure and pressure derivative curves, the unique characteristics of the different flow regimes resulting from partially penetrating wells in naturally fractured and un-fractured homogenous reservoir. The interpretation of pressure response tests were done using Tiab's direct synthesis (TDS) technique for analyzing log-log plot of pressure and pressure derivative.

Igbokoyi and Tiab (2007) developed new type curves for well test analysis for non-Newtonian power law fluids in porous media using the general analytical solution in Laplace variable presented by Ikoku and Ramey Jr. (1978) as the mathematical basis of the proposed type curves, and the Tiab's direct synthesis (TDS) technique of evaluating well test data for non-Newtonian fluid flow in porous media was developed.

More recently, Igbokoyi and Tiab (2010) presented a new method of estimating permeability anisotropy for transient well test data in naturally fractured reservoir using elliptical flow model. Pressure and pressure derivative type curves were developed and the plots showed that if radial flow model is used

for interpretation, the early linear flow regime observed could be erroneously interpreted as wellbore storage effect.

The review of petroleum literature over the last four decades shows that authors have paid little attention to spherical flow of fluids in petroleum reservoir. Although quite a number of works have been done on pressure transient behaviour of non-Newtonian power-law fluid flow in porous media assuming linear and radial flow pattern, none has been published on pressure transient analysis for spherical flow behaviour of non-Newtonian power-law fluid in homogenous and naturally fractured reservoir system.

1.3 Problem Statement

Polymer flooding operations on field works have been reported successful, but most of the time their well test data analysis have not yielded satisfactory results. Some of the reasons for the unsatisfactory results are:

i. Erroneous interpretation of non-Newtonian rheology exhibited by the injected polymer fluid
ii. The distribution of polymer fluid within the reservoir, which is usually unknown
iii. Erroneous assumption of radial flow pattern of fluid into the wellbore of a thick reservoir with small completion interval/limited-entry open to flow, or wellbores with partial penetration.

Furthermore, for a draw-down/build-up test, the use of Newtonian fluid model for the analysis of the well-test data may be erroneous for high viscosity crude which by their nature may exhibit Non-Newtonian flow behaviour.

Moreover, for the aforementioned reasons, authors have carried out abundant studies on non-Newtonian power-law fluid behaviour in porous media, but its spherical flow pressure transient behaviour in porous media is yet to be published.

Therefore, this work presents non-Newtonian power-law fluids pressure behaviour in Homogenous and Naturally Fractured Reservoir with spherical flow.

Chapter 2

Spherical Flow Model for Homogenous Reservoir

2.1 Spherical Flow Description in Partially Penetrating/Limited-entry Wells

It has been reported abundantly in literature that spherical flow behaviour characterize wells with limited-entry, partial completion and penetration in reservoirs with thick formation. Below are some diagrammatic descriptions of spherical flow in vertical wells completed in thick formation reservoirs.

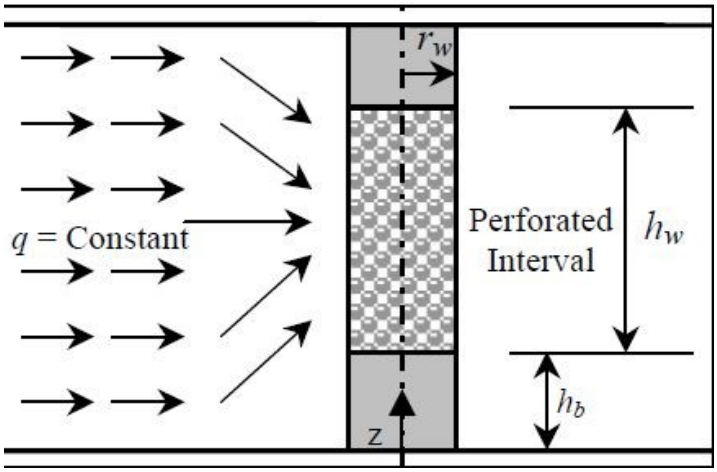

a. Limited-entry completion Well characterized with Spherical flow

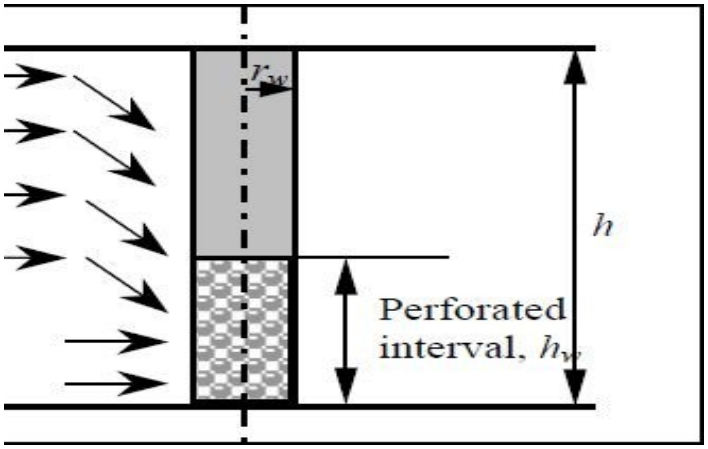

b. Well partially penetrating at the bottom characterized with Spherical flow

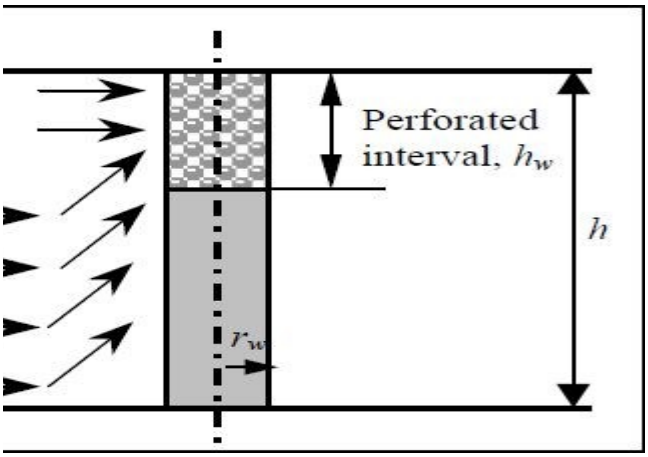

c. Well partially penetrating at the top characterized with Spherical flow

Fig.2.1.1 Different types of partially penetrating Wells in thick formation reservoir (Sonatrach et al. 2006)

2. 2 Mathematical Model Assumption and Development

This section outlines stepwise method of developing mathematical model for Pressure transient behaviour of power-law fluids in Homogenous using mathematical model assumptions.

2.2. 1 Model Assumption

- Homogenous Isotropic formation
- Steady state effective viscosity
- Laminar and Darcy's flow is valid
- The fluid is isothermal, single phase and slightly compressible with constant properties
- Fluid flows into the wellbore spherically
- Infinite acting behaviour is experienced.

2.2.2 Model Development

Continuity equation of slightly compressible fluids for spherical flow in porous media, as presented by Liu Ci-qun, is:

$$\phi c_t \frac{\partial P}{\partial t}$$

(1)

But flow, v_r for non-Newtonian power-law fluids in porous media is:

(2)

Thus, the continuity equation for spherical flow of non-Newtonian power-law fluids is:

$$= n\phi c_t \frac{\partial P}{\partial t}$$

(3)

And the diffusivity equation for spherical flow of non-Newtonian power-law fluid is:

$$\left] = \left(\frac{n\phi c_t \mu_{eff}}{k} \right) \left(\frac{q}{2\pi} \right)^{n-1} r^{2(1-n)} \frac{\partial P}{\partial t} \right.$$

(4)

The diffusivity equation in dimensionless terms is:

$$\left. \frac{\partial P_D}{\partial r_D} \right] = r_D^{\,2(1-n)} \frac{\partial P_D}{\partial t_D}$$

(5)

$$\frac{k}{r_w \mu_{eff}} (P_i - P)$$

Where,
(6)

(7)

(8)

$$\overline{\ ^{2}_{w}}$$

(9)

The dimensionless initial and boundary conditions are:

(10)

(11)

$$\left(1 - C_D \frac{\partial P_{wD}}{\partial t_D}\right)$$

(12)

$$\frac{\partial P}{\partial t_D}\Big)_{r_D=1}$$

(13)

The linearized form of equation (5)

$$= r_D^{\,2(1-n)} \frac{\partial P_D}{\partial t_D}$$

(14)

Taking the Laplace of equation (14) gives:

$$- s\overline{P_D} r_D^{\,2(1-n)} = 0$$

(15)

The solution of equation (15) in Laplace space is:

$$\frac{K_V\left(\alpha\sqrt{s}\right)}{sK_\beta\left(\alpha\sqrt{s}\right)}$$

(16)

But equation (16) is the dimensionless wellbore pressure without skin and wellbore storage. The dimensionless wellbore pressure with skin and wellbore storage incorporated is:

$$\frac{K_V\left(\alpha\sqrt{s}\right)+S\sqrt{s}K_\beta\left(\alpha\sqrt{s}\right)}{K_\beta\left(\alpha\sqrt{s}\right)+sC_D\left[K_V\left(\alpha\sqrt{s}\right)+S\sqrt{s}K_\beta\left(\alpha\sqrt{s}\right)\right]\right]}$$

(17)

Where,

For Newtonian fluid (i.e. n=1) spherical flow behaviour, equation (17) becomes:

$$\frac{K_{\frac{1}{2}}\left(\sqrt{s}\right)+S\sqrt{s}K_{\frac{3}{2}}\left(\sqrt{s}\right)}{K_{\frac{3}{2}}\left(\sqrt{s}\right)+sC_D\left[K_{\frac{1}{2}}\left(\sqrt{s}\right)+S\sqrt{s}K_{\frac{3}{2}}\left(\sqrt{s}\right)\right]\right]}$$

(18)

And for the case n=0.5 equation (17) reduces to pseudo radial flow behaviour which is:

$$\frac{K_0\left(\frac{2}{3}\sqrt{s}\right)+S\sqrt{s}K_1\left(\frac{2}{3}\sqrt{s}\right)}{K_1\left(\frac{2}{3}\sqrt{s}\right)+sC_D\left[K_0\left(\frac{2}{3}\sqrt{s}\right)+S\sqrt{s}K_1\left(\frac{2}{3}\sqrt{s}\right)\right]\right]}$$

(18a)

Liu Ci-qun presented an analytical Laplace inversion solution of equation (16) without skin (i.e. S=0) as:

$$\frac{-2n)^{2V}t_D{}^V}{2n)\Gamma\left(\frac{3}{4-2n}\right)}-\frac{1}{1-2n}$$

(19)

For the case with skin, analytical solution is:

$$\frac{-2n)^{2V} t_D{}^{V}}{2n)\Gamma\left(\frac{3}{4-2n}\right)} - \frac{1}{1-2n} + S$$

(20)

The equation (20) above is the analytical solution for the long-time approximation for all flow behaviour index of power-law fluids except for n=0.5, in which the above equation is not valid. Therefore the solutions for case when n=0.5 are:

S

(20a)

Equation (20a) is the early time solution. The late time approximate solution is:

$$\frac{\gamma}{3} + \frac{2\ln 3}{3} + S$$

(20b)

Therefore, for a spherical Non-Newtonian flow, the long time pressure derivative is 0.33 when n = 0.5.

(20c)

Furthermore, the long time approximate solutions obtained at S=0, for all cases of flow behaviour index, does not give the exact same value of Dimensionless pressure as the Numerical solution. This is due to

omission of the sum of function, , as suggested by Ikoku (1978) and Odeh

et al. (1979), in the long time analytical solutions obtained; where is a function of

flow behaviour index (n). Empirical investigations carried out in this study suggest that

is a small value function and it's bounded mathematically as:

$$\left(\frac{\partial}{\partial}\right) > 0$$

(For all flow behaviour index values of power-law fluids)

2.3 Type Curve Development

In developing Dimensionless Pressure Type curve, Stehfest algorithm is used to invert equation (17). The equation parameters are supplied into the algorithm and different Dimensionless Pressure Type curves are generated for various skin factor and flow behaviour index (n=0.2-0.8) of power-law fluids. Furthermore, Dimensionless Pressure derivative Type curves are developed for various skin and flow behaviour index of power-law fluid using the same Stehfest algorithm to invert the derivative form of equation (17). The derivative form of equation (17) is:

$$\frac{K_V\left(\alpha\sqrt{s}\right) + S\sqrt{s}K_\beta\left(\alpha\sqrt{s}\right)}{K_\beta\left(\alpha\sqrt{s}\right) + sC_D\left[K_V\left(\alpha\sqrt{s}\right) + S\sqrt{s}K_\beta\left(\alpha\sqrt{s}\right)\right]\Big]}$$

(21)

The different Pressure and Pressure derivative Type curves are generated on MATLAB simulation platform. The effect of wellbore storage is incorporated in the developed Type curves.

2.4 Type Curves

This section gives the summary of developed type curves. Figure 2.4.1 shows the dimensionless Pressure Type curve for the case S = 0 and C_D = 0, for some values of flow behaviour index (n= 0.2 – 1.0).

Figure 2.4.2 is the Pressure and Pressure derivative Type curve for the case S = 2 for various flow behaviour index (n= 0.2 – 1.0). Figure 2.4.3-2.4.9 are the plots of Pressure derivative for skin factor S = 2-10 for various flow behaviour index (n=0.1-1.0).

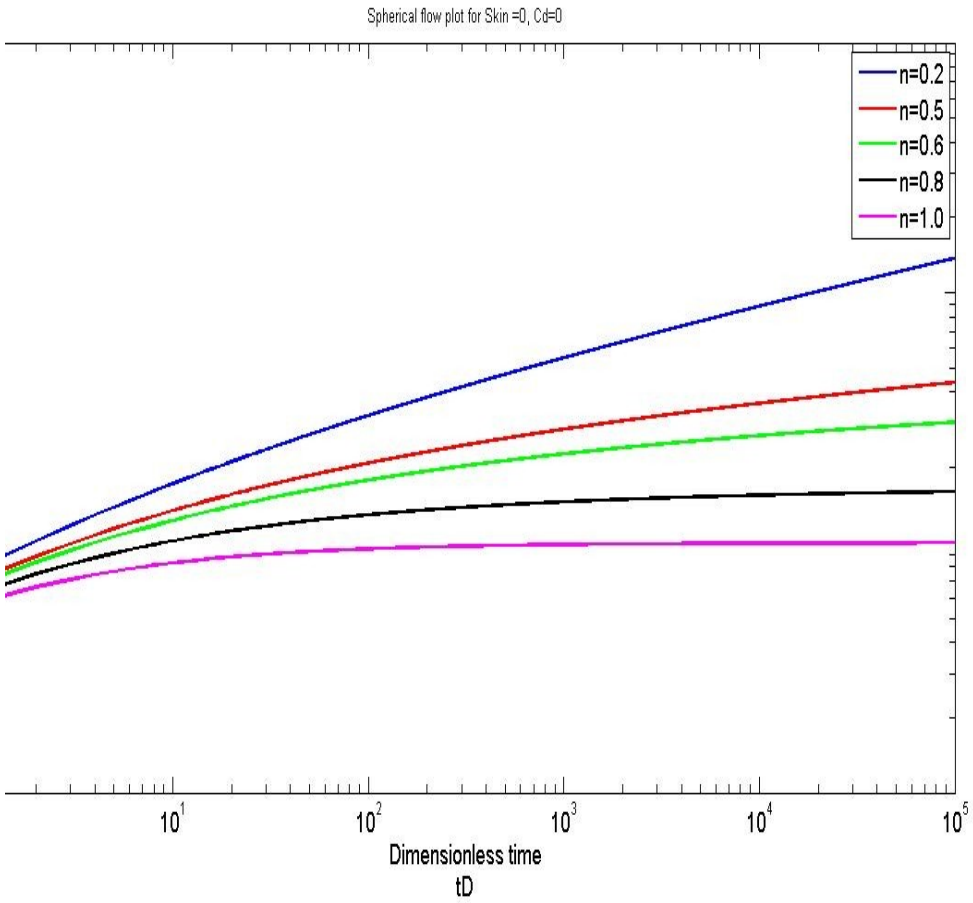

Fig.2.4.1 Dimensionless Pressure Plot of Spherical flow behaviour of power-law fluid in Homogenous Reservoir system for Skin = 0 & $C_d = 0$

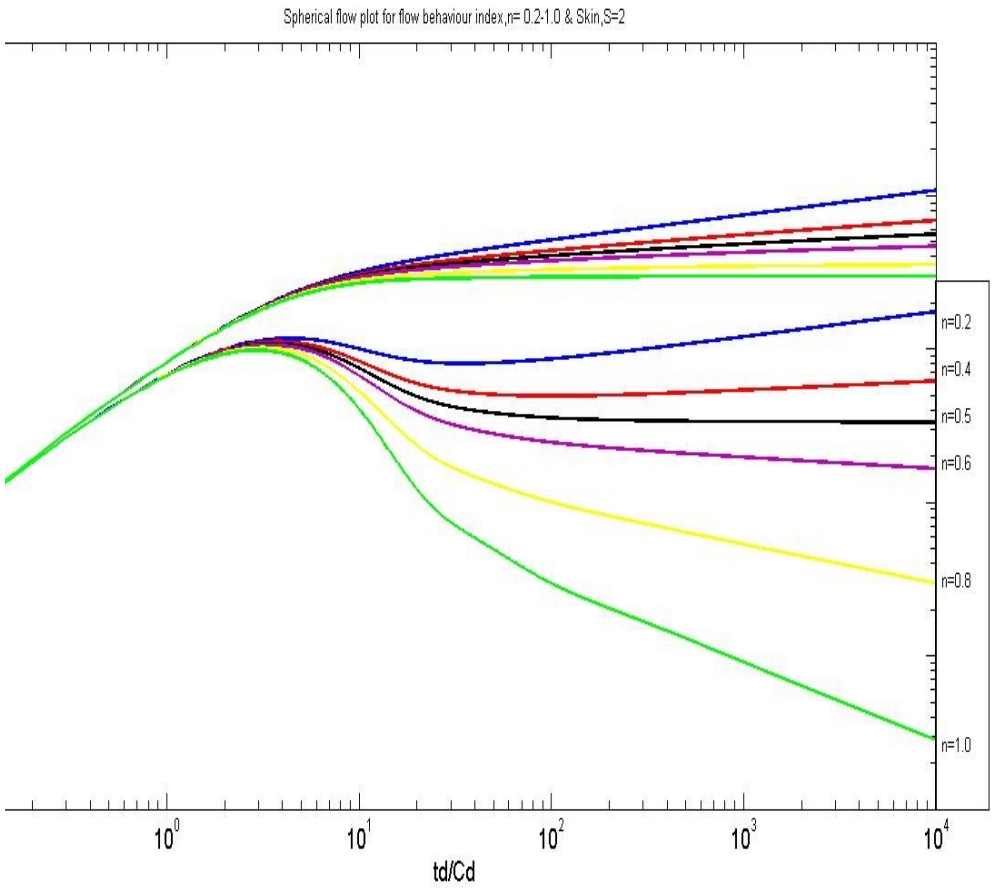

Fig.2.4.2a Pressure and Pressure derivative plot of Spherical flow behaviour of power-law fluid in Homogeneous Reservoir system for n=0.2-1.0 & Skin =2

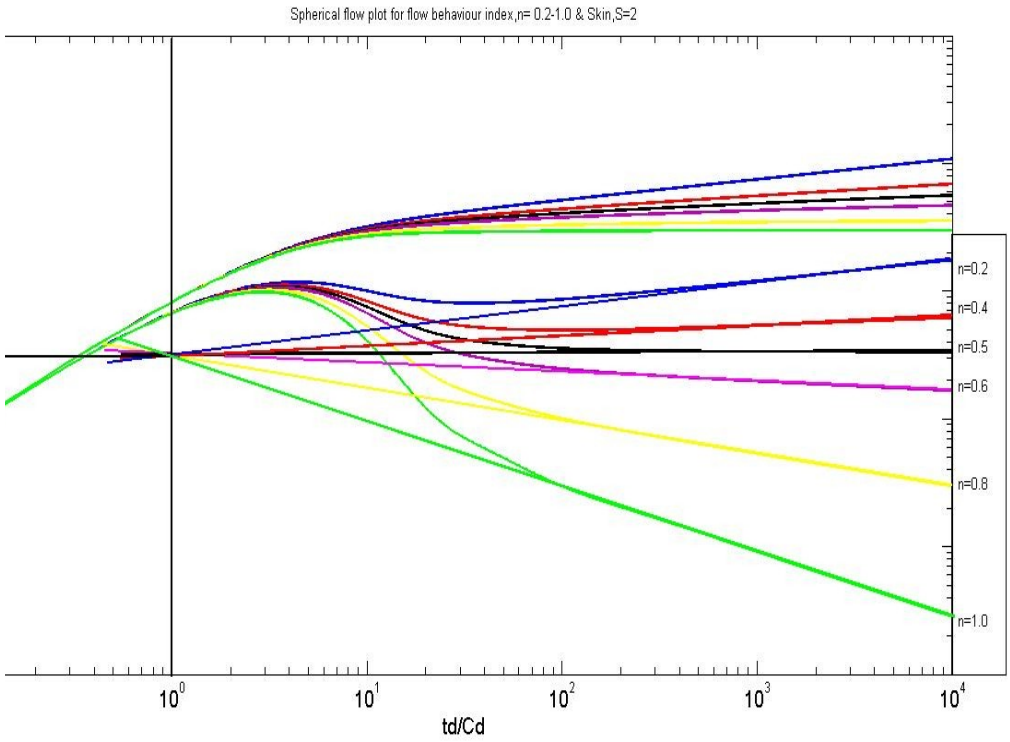

Fig.2.4.2b Plot of Pressure derivative straight line intersecting 0.3 line at $t_D/C_D = 1$

The deduction in the figure above is rounded-up from the pressure derivative of the long time approximate solution. This is developed as follows:

Long-time pressure derivative solution is:

$$\frac{(4-2n)^{2V-1}}{\left(\frac{3}{4-2n}\right)}\left(\frac{t_D}{C_D}\right)^V$$

Therefore at, a weighted average pressure derivative value of 0.3117 is obtained from the long time approximate solution for all flow behaviour index values, n, of power-law fluid. This is shown in the appendix, Table A-2). Thus, the general representation for pressure derivative at $t_D/C_D = 1$ for all flow behaviour index values of power-law fluid can be expressed as:

$$\frac{(4-2n)^{2V-1}}{\Gamma\left(\frac{3}{4-2n}\right)} \approx 0.3$$

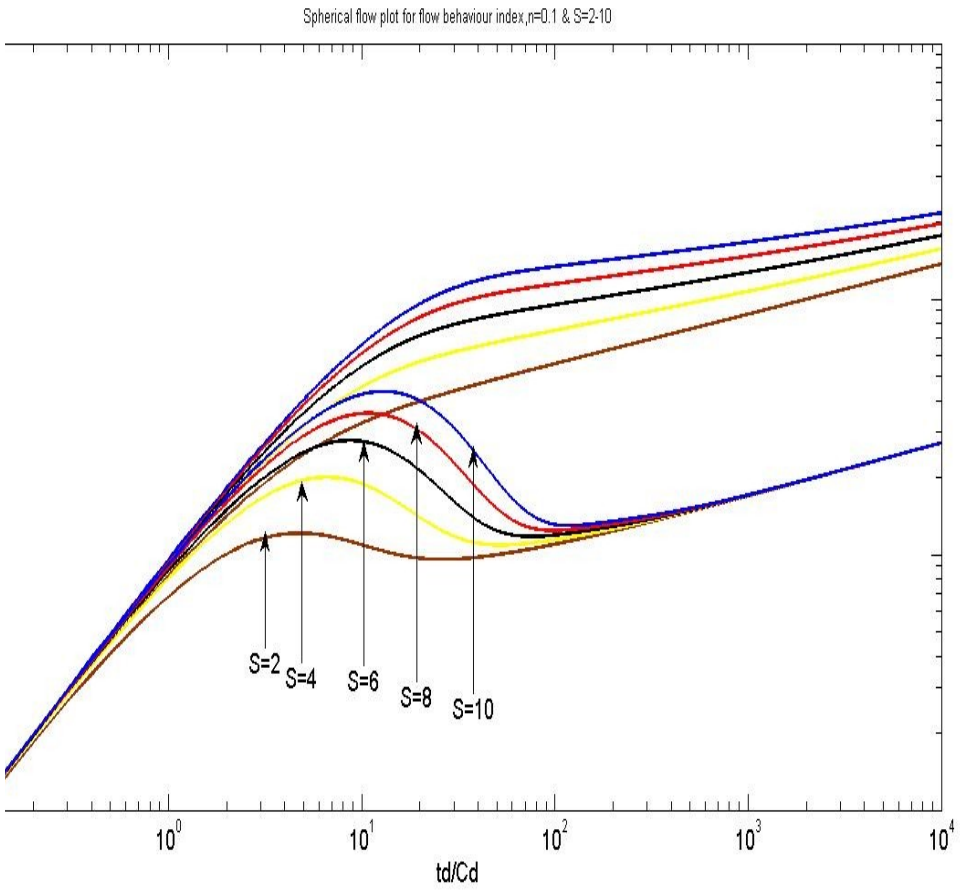

Fig.2.4.3 Pressure and Pressure derivative plot of Spherical flow behaviour of power-law fluid in Homogeneous system for n=0.1 & Skin =2-10

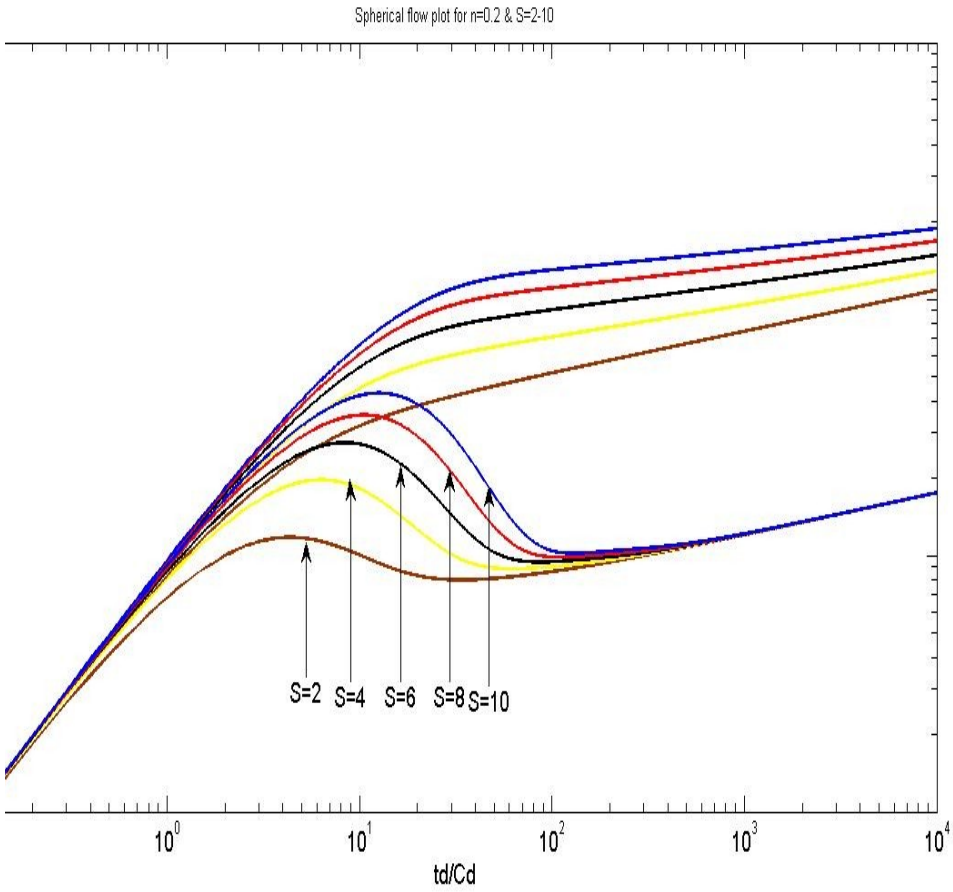

Fig.2.4.4 Pressure and Pressure derivative plot of Spherical flow behaviour of power-law fluid in Homogeneous system for n=0.2 & Skin =2-10

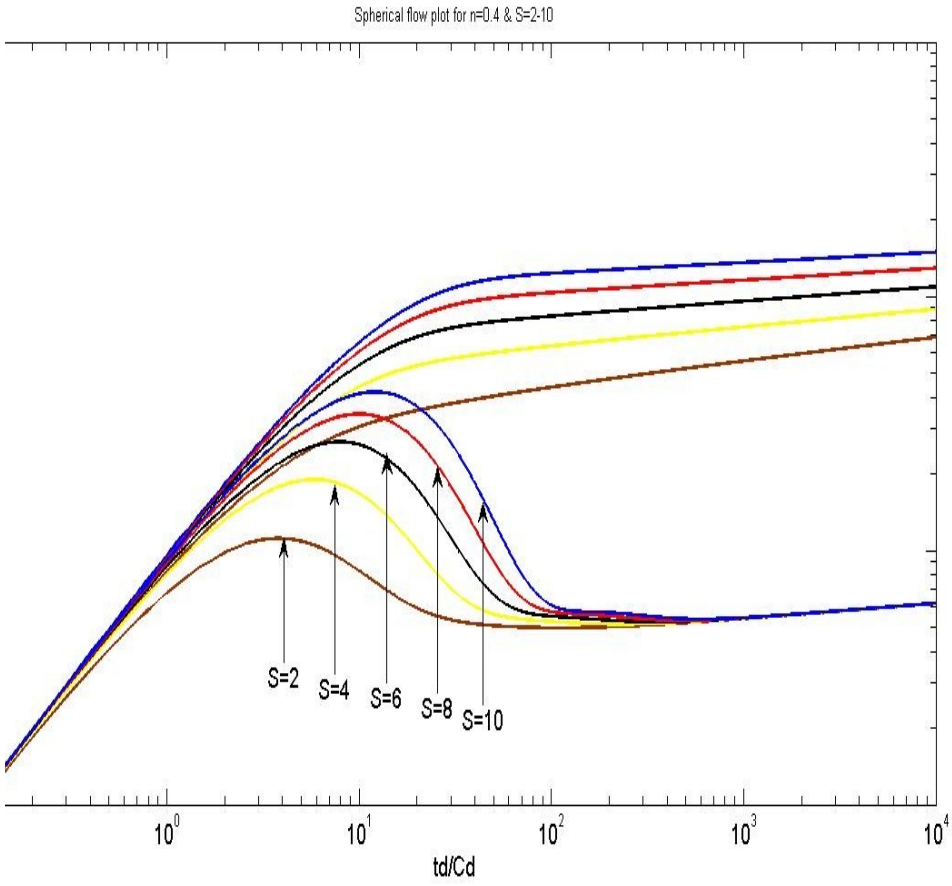

Fig.2.4.5 Pressure and Pressure derivative plot of Spherical flow behaviour of power-law fluid in Homogeneous system for n=0.4 & Skin = 2-10

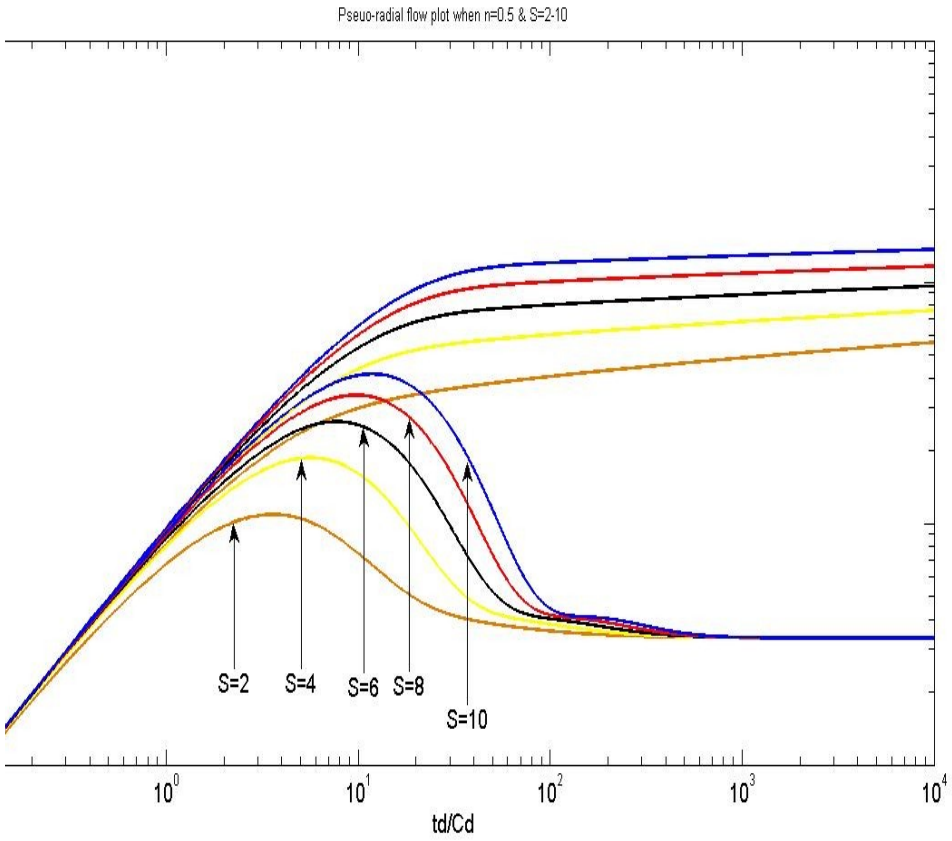

Fig.2.4.6 Pressure and Pressure derivative plot of Spherical flow behaviour of power-law fluid in Homogeneous system for n=0.5 & Skin =2-10

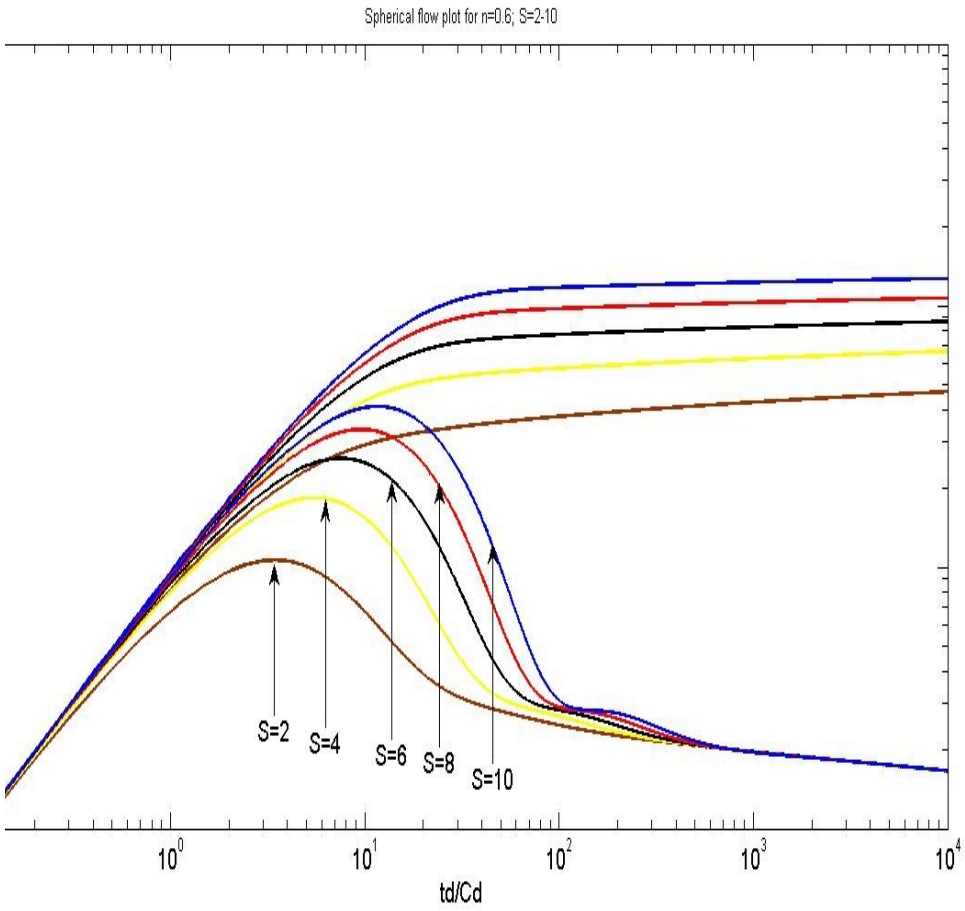

Fig.2.4.7 Pressure and Pressure derivative plot of Spherical flow behaviour of power-law fluid in Homogeneous system for n=0.6 & Skin = 2-10

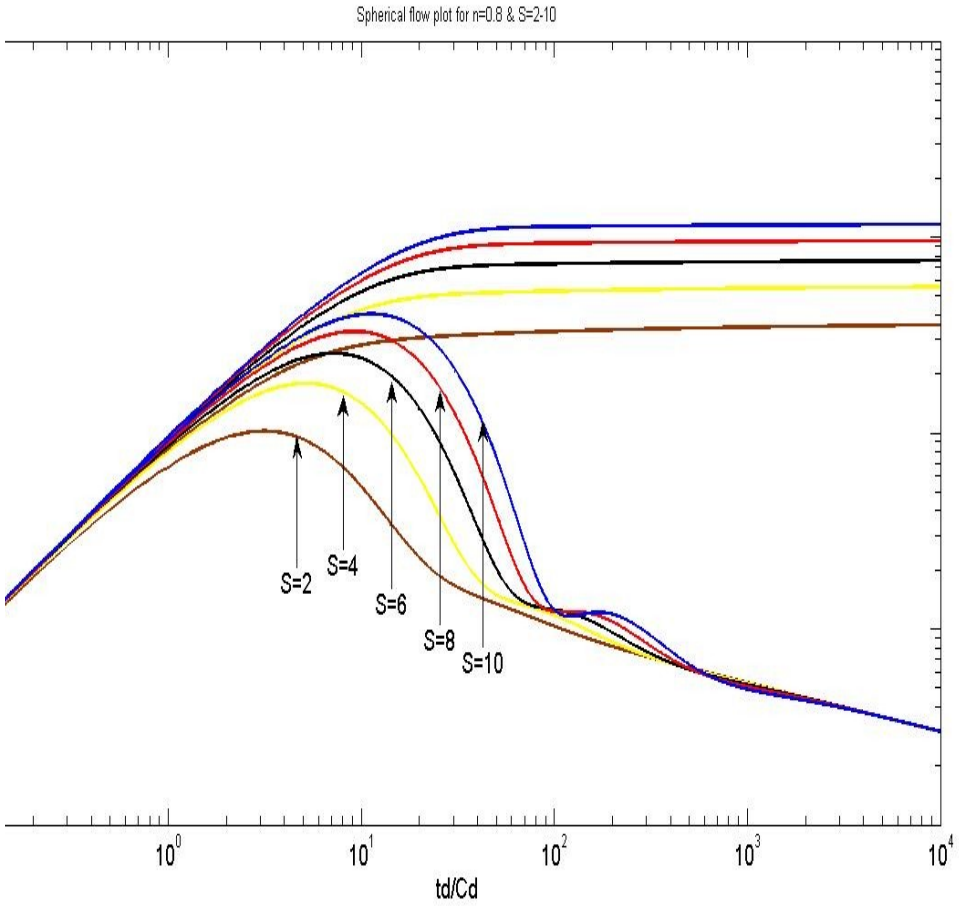

Fig.2.4.8 Pressure and Pressure derivative plot of Spherical flow behaviour of power-law fluid in Homogeneous system for n=0.8 & Skin =2-10

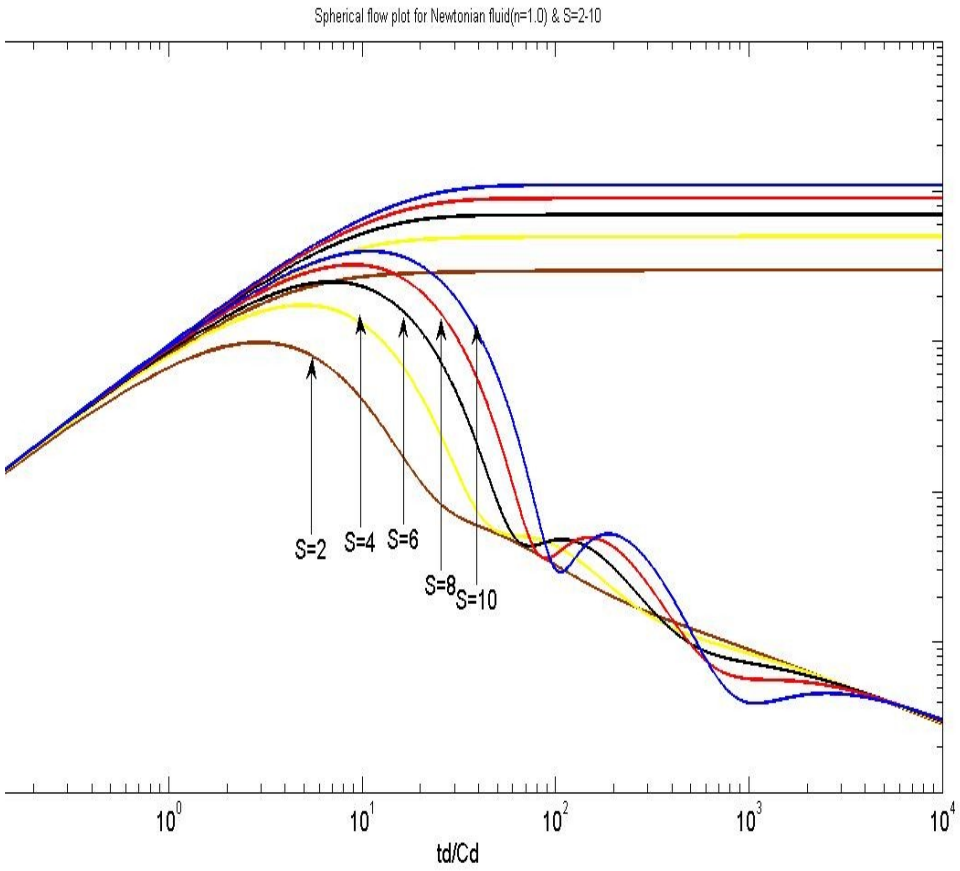

Fig.2.4.9 Pressure and Pressure derivative plot of Spherical flow behaviour of power-law fluid in Homogeneous system for n= 1.0 & Skin =2-10

2.5 Estimating Reservoir and Wellbore Parameters

2.5.1 The Method of Type Curve Matching

Resolving equation (6), fluid mobility can be estimated as:

$$\left(\frac{k}{\mu}\right)_{eff} = r_w^2 \left(\frac{P_D}{\Delta P}\right)_{TCM}$$

(22)

Subscript TCM represents Type curve match

Dividing equation (7) by (9), wellbore storage can be estimated as:

$$C = \frac{k}{\mu_{eff}} \left[\frac{t}{t_D / C_D}\right]_{TCM}$$

(23)

Permeability *k* can be estimated from equation (22) above by providing the effective viscosity, which is often estimated from relationship developed by Blake Kozeny (Gidley et al. (1989)):

$$\mu_{eff} = \left[\frac{\left(3 + \frac{1}{n}\right)^n 3^{n+1} d_p^{\,1-n} \phi^{2(1-n)}}{75(1-\phi)^{1-n}}\right]$$

(24) Also flow behaviour index (n) and skin (S) can be determined from the corresponding Type curve match.

2.5.2 Tiab's Direct Synthesis Technique (TDS)

This technique uses a log-log plot of Pressure and Pressure derivative against time to show the characteristic finger-prints unique to Pressure behaviour. The method further develops equations from analytical solution of the long time approximation and the pressure derivative plot to estimate Wellbore and Reservoir parameters. Thus, differentiating the analytical solution of the long time approximation developed in equation (20)

$$\frac{4-2n)^{2V}}{)\Gamma\left(\frac{3}{4-2n}\right)}t_D{}^{V-1}$$

(25a)

Multiplying equation (25a) by t_D

$$\frac{2n)^{2V-1}}{\frac{3}{4-2n}}t_D{}^{V}$$

(25b)

Substituting the dimensionless terms from equation (7) and the differential of (6) into (25b), mobility can be obtained as:

$$\left[\frac{:V-1}{\left(\frac{t_{sp}}{n\phi c_t}\right)^{V}\left(\frac{2\pi}{q}\right)^{\frac{1+n}{2n-4}}\frac{1}{\left(\Delta P_w{}'\times t\right)_{sp}}}\right]^{\frac{1}{1-V}}$$

(26)

Subscript sp denotes the straight line region of the pressure derivative plot i.e. the spherical flow region.

Substituting equation (25b) into (20):

$$\frac{:P_{wD}{}')}{V}-\frac{1}{1-2n}+S$$

; From this expression the skin factor S can be estimated by substituting the dimensionless terms into the expression

$$\frac{k}{r_w^{1-2n}}\left[(\Delta P_w)_{sp}-\frac{(\Delta P_w\times t)_{sp}}{V}\right]+\frac{1}{1-2n}$$

(27)

The equation (27) above for determining skin factor for different values of flow behaviour index is not valid when n=0.5; hence for the case when n=0.5, skin factor can be estimated from the long-time analytical solution of equation (20b) as:

$$\frac{(\Delta P_w)_{sp}}{\mu_{eff}}\right]-0.3\ln\left[\left(\frac{2\pi}{q}\right)^{0.5}\frac{t_{sp}k}{0.5\phi c_t\mu_{eff}}\right]-0.54$$

(27a)

, are read from the Pressure and Pressure derivative plot at the spherical flow straight line.

From the log-log plot of Pressure derivative, the straight line equation of the spherical flow region can be expressed as:

$$\left(\frac{}{_D}\right)=V\log\left(\frac{t_D}{C_D}\right)+\log\left[\frac{(4-2n)^{2V-1}}{\Gamma\left(\frac{3}{4-2n}\right)}\right]$$

(28) In the above equation, it can be deduced that the slope of the Pressure derivative straight line is V.

Recall, ; hence Flow behaviour index, can be determined from this as:

(29)

Likewise, the Pressure derivative straight line gives a value of 0.3 when extrapolated to

(this is shown in Fig.2.4.2b and further clarified in the appendix, Table A – 2,

0.3

using approximate solution); thus gives the general representation of pressure derivative at $t_D/C_D = 1$ for all flow behaviour index values of power-law fluid. Therefore at

Equation (28) becomes:

$$\left.\right]_{TCM} = 0.3$$

(30)

Substituting the dimensionless terms into the above expression, mobility can be expressed as:

$$\frac{r_w^{1-2n}}{t)_{TCM}}$$

(31)

$$0.3\left(\frac{t_D}{C_D}\right)^{V}$$

Equation (25b) can also be written as:

Substituting the dimensionless terms, mobility can also be estimated as:

$$\overline{t}_{sp}\left[\left(\frac{2\pi h r_w^{\,2} t_{sp}}{C}\right)^{V}\left(\frac{2\pi}{q}\right)^{\frac{1+n}{2n-4}}\right]^{\frac{1}{1-V}}$$

(32)

Simplifying equation (26) by substituting 0.3 for , the equation becomes:

$$\overline{t}_{sp}\left[\left(\frac{t_{sp}}{n\phi c_t}\right)^{V}\left(\frac{2\pi}{q}\right)^{\frac{1+n}{2n-4}}\right]^{\frac{1}{1-v}}$$

(33)

It has been shown that at early time the log-log plot Pressure and Pressure derivative has a unit slope due to the predominant effect of wellbore storage. Therefore at early time, estimate of wellbore storage can be determined.

Combining equation (6), (7) and (9), an expression for determining wellbore storage can be developed.

$$\left(\frac{\quad}{\quad}\right)_e \qquad \left(\frac{t}{t'\times t}\right)_e$$

or

(34)

Subscript e represents a coordinate on the unit slope line.

Step by step procedure of applying TDS technique

- Compute the pressure difference for Injection or Falloff test and the

pressure derivative

- Plot on a log-log scale & versus injection time for

Injection test or for Falloff test

- Identify the unit slope line at the early time of the plot representing the wellbore storage effect. Quantify the wellbore storage effect using equation (34)

- Identify the derivative straight line region (spherical flow region) on the plot and determine its slope V; from this obtain the flow behaviour index of the power-law fluid using equation (29)

- Select any values of , and

in the spherical flow region of the plot; compute using equation

(32) or (33). Equation (24) can be used to estimate , thus can be determined

- Compute skin factor using equation (27) or (27a) for n=0.5.

Chapter 3

Spherical Flow Model for Naturally Fractured Reservoir

3.1 Mathematical Model Assumption and Development

This section outlines stepwise method of developing mathematical model for Pressure transient behaviour of power-law fluids in Naturally Fractured Reservoir using mathematical model assumptions.

3.1.1 Model Assumption

- Steady state effective viscosity
- Homogenous Isotropic formation (matrix and fracture each has uniform properties)
- Slightly compressible isothermal fluid with single phase flow in both the matrix and fracture
- Reservoir is at the same initial reservoir pressure at time t = 0
- Fluid flows into the wellbore spherically
- Fracture provides the essential permeability of fluid flow into the wellbore
- Darcy's law is valid for fluid flow near the wellbore
- Pseudo-steady state inter-porosity fluid (Warren and Root model).

3.1.2 Model Development

The continuity equation for power-law fluid flow through the fracture in NFR can be written as:

$$\frac{k_f}{u_{eff}} \frac{\partial P_f}{\partial r} \left] = n[\phi c_t]_f \frac{\partial P_f}{\partial t} - q \right.$$

(35) and for flow in matrix we have:

$$\frac{k_m}{u_{eff}} \frac{\partial P_m}{\partial r} \left] = n[\phi c_t]_m \frac{\partial P_m}{\partial t} + q \right.$$

(36) Assuming pseudo-steady state flow from matrix to fracture

$$\frac{P_m}{)t}$$

(37)

Substituting equation (38) into (36):

$$= \left(\frac{n\mu_{eff}}{k_f} \right) \left(\frac{q}{2\pi r^2} \right)^{n-1} \left[\left[\phi c_t \right]_f \frac{\partial P_f}{\partial t} + \left[\phi c_t \right]_m \right]$$

(38)

The dimensionless definition of equation (38) is:

$$\frac{\partial P_{fD}}{\partial r_D} \right] = r_D^{2(1-n)} \left[\omega \frac{\partial P_{fD}}{\partial t_D} + (1-\omega) \frac{\partial P_{mD}}{\partial t_D} \right]$$

(39)

Where,

$$\frac{k_j}{\mu_{eff} r_w} \left(P_i - P_j \right)$$

(40) Subscript j = f or m, the indices for fracture (f) and (m)

$$\frac{q}{2\pi} \left(\left[\phi c_t \right]_f + \left[\phi c_t \right]_m \right)$$

;

(41)

;

(42)

Warren and Root presented Matrix-Fracture interface condition as:

$$P_f \right)$$

(43) Equating equation (43) to (37) we have:

$$= \frac{\gamma k_m}{\mu_{eff}} \left(P_m - P_f \right)$$

(44) The dimensionless form of equation (44) is:

$$P_{fD} - P_{mD}\Big)$$

(45)

In which,

$$\frac{q}{\tau r_w^{\,2}}\Big)^{n-1} \div \Big) \qquad\qquad \overline{c_t}\Big]_m$$

;

(46)

Taking the Laplace transform of equation (39) and (45) we obtain:

$$\frac{\partial \overline{P_{fD}}}{\partial r_D}\Big] = r_D^{\,2(1-n)}\Big[\omega s\overline{P_{fD}} + (1-\omega)s\overline{P_{mD}}\Big]$$

(47)

$$\overline{P_{fD}} - \overline{P_{mD}}\Big)$$

(48)

Re-arranging equation (48) and substituting into (47) diffusivity equation for NFR is:

$$\frac{\partial \overline{P_{fD}}}{\partial r_D}\Big] = r_D^{\,2(1-n)} sf(s)\overline{P_{fD}}$$

(49)

$$\frac{)s+\lambda}{)+\lambda}$$

Following the general procedure for applying Homogenous solution to Double porosity system, the Laplacian space solution of spherical flow behaviour of power-law fluid in NFR can be written as:

$$\frac{K_V\left(\alpha\sqrt{sf(s)}\right)}{\overline{(s)}K_\beta\left(\alpha\sqrt{sf(s)}\right)}$$

(50)

Incorporating skin and wellbore storage effect, the above equation becomes:

$$\frac{K_V\left(\alpha\sqrt{sf(s)}\right)+S\sqrt{sf(s)}K_\beta\left(\alpha\sqrt{sf(s)}\right)}{\left(\alpha\sqrt{sf(s)}\right)+sC_D\left\{\left(K_V\left(\alpha\sqrt{sf(s)}\right)+S\sqrt{sf(s)}K_\beta\left(\alpha\sqrt{sf(s)}\right)\right)\right\}\Big]}$$

(51)

To develop the solutions of the above equations, for purpose of interpretation, the Laplace inversion of equation (50) will be done analytically while (51) will be done numerically.

Therefore the early time solution of equation (50) with skin factor incorporated is:

$$\frac{2n)^{2V}}{\Gamma\left(\frac{3}{4-2n}\right)}\left(\frac{t_D}{\omega}\right)^{V}-\frac{1}{1-2n}+S$$

(52a)

And the late time solution is:

$$\frac{2n)^{2V}}{\Gamma\left(\frac{3}{4-2n}\right)}t_D{}^{V}-\frac{1}{1-2n}+S$$

(52b)

But equations (52a) & (52b) above are only valid for all flow behaviour index values except n=0.5. Hence its early and late time solutions, without skin, are given below

The early time and late time solutions respectively:

$$\frac{\gamma}{3}+\frac{2\ln 3}{3}$$

;

(53c)

3.2 Pressure and Pressure derivative Type Curve Development

Stehfest Algorithm is used to invert equation (51) and Pressure and Pressure and Pressure derivative Type curves are plotted for different flow behaviour index, inter-porosity flow parameters and various

dimensionless storage coefficient values at a constant skin factor. Figure (3.2.1) shows the dimensionless Pressure derivative plot for various flow behaviour index (n= 0.2-1.0) at a constant value of inter-porosity flow parameter (λ= 0.001), dimensionless storage coefficient (ω= 0. 1) and skin factor (S=2). Figure (3.2.2) & (3.2.3) show the Pressure derivative plot for different values of dimensionless storage coefficient (ω = 0.001-1.0) and different values of inter-porosity flow parameter respectively for a flow behaviour index (n = 0.2) while other parameters are kept constant. The subsequent plots (Figure (3.2.4) – (3.2.11)) follow the same trend for various values of flow behaviour index.

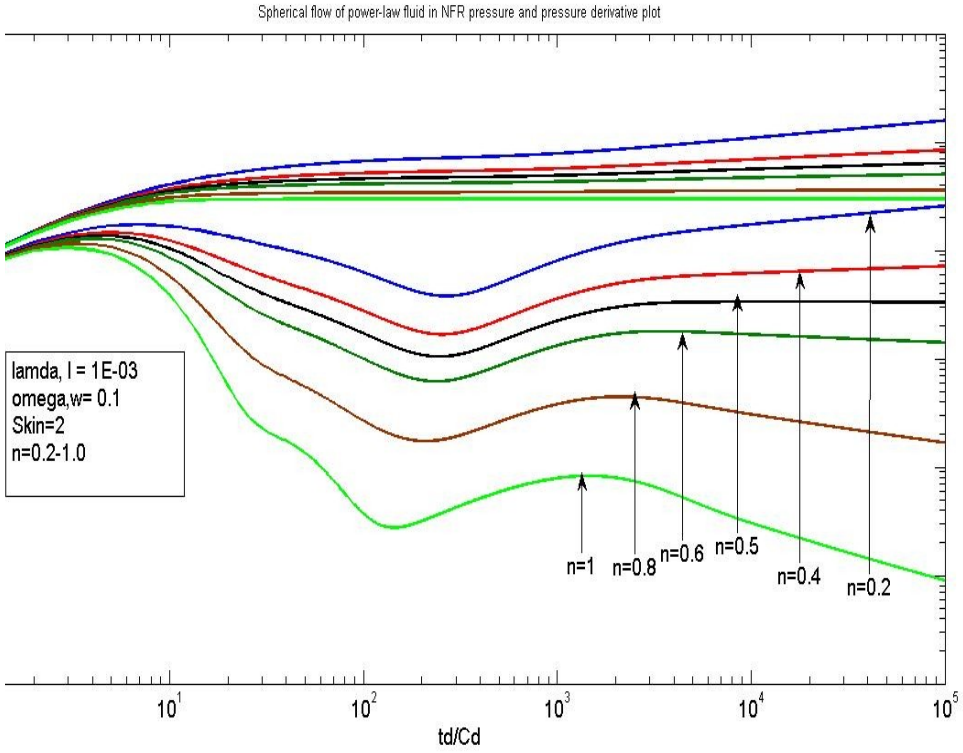

Fig.3.2.1 Pressure and Pressure derivative plot for Spherical flow behaviour of power-law fluid in NFR. (Skin=2; lambda, λ= 1E-03; omega, ω=0.1)

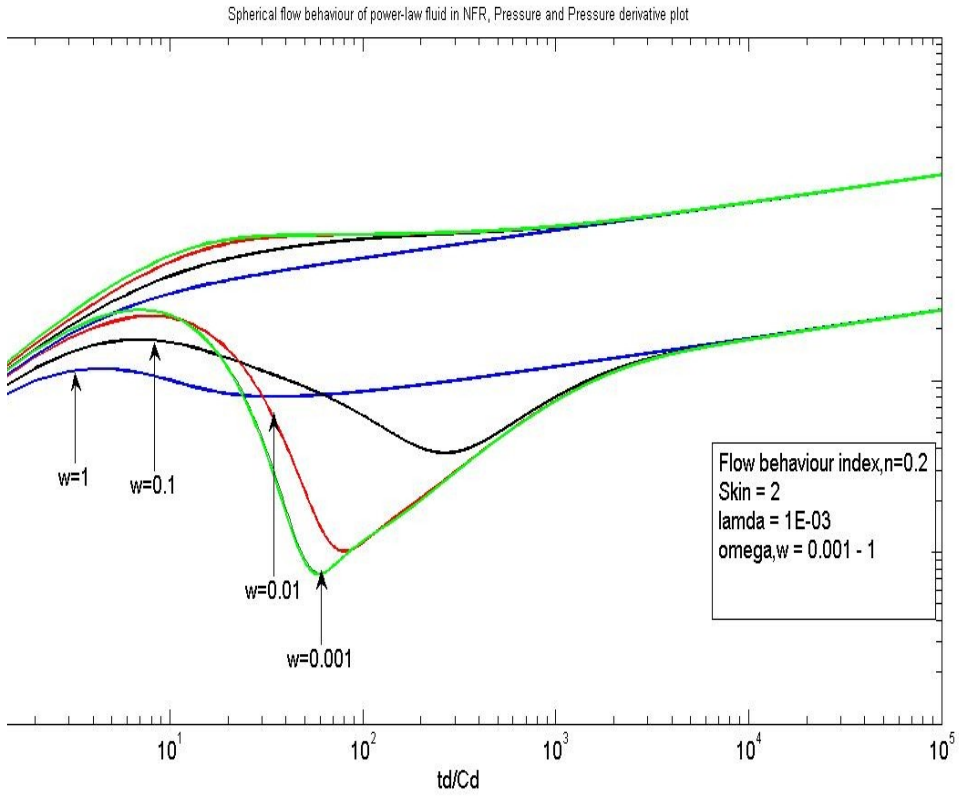

Fig.3.2.2 Pressure and Pressure derivative plot for Spherical flow behaviour of power-law fluid in NFR. (Skin=2; lambda, λ= 1E-03; omega, n=0.2)

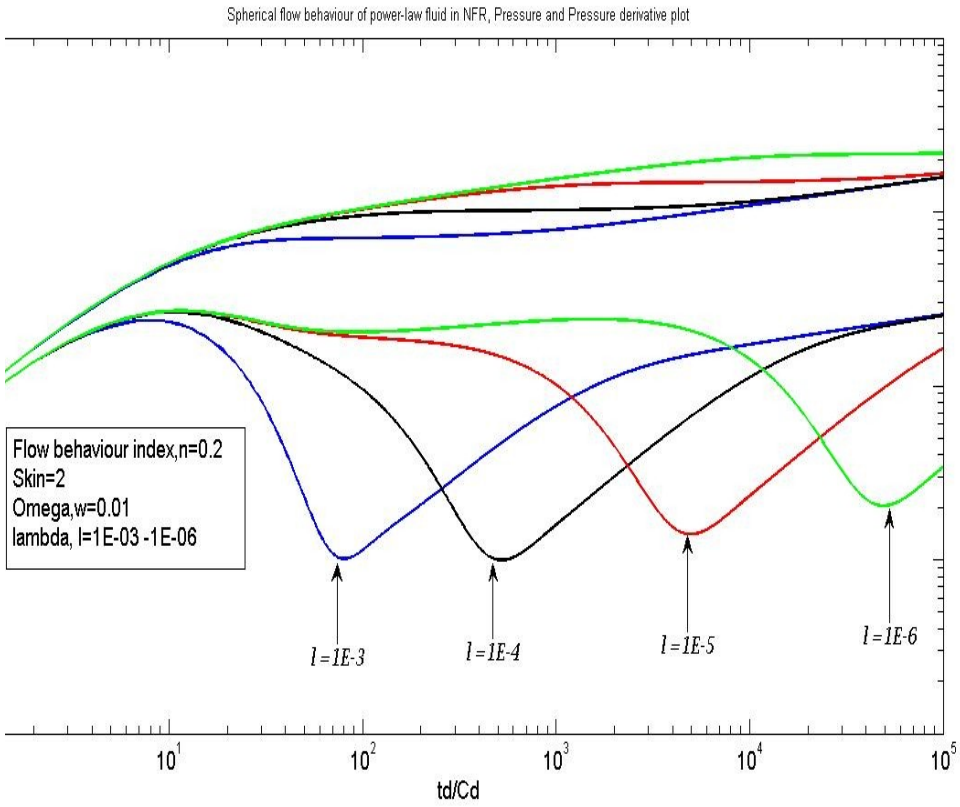

Fig.3.2.3 Pressure and Pressure derivative Spherical flow behaviour of power-law fluid in NFR. (Skin=2; omega, ω= 1E-02; n=0.2)

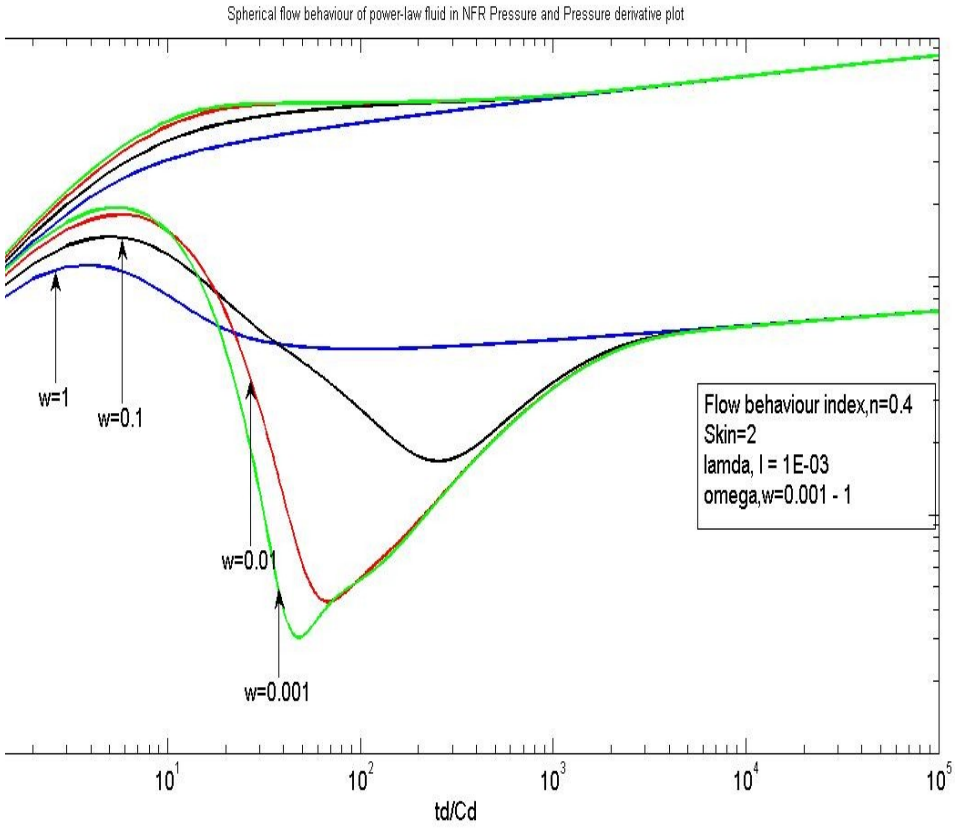

Fig.3.2.4 Pressure and Pressure derivative plot for Spherical flow behaviour of power-law fluid in NFR. (Skin=2; lambda, λ= 1E-03; omega, n=0.4)

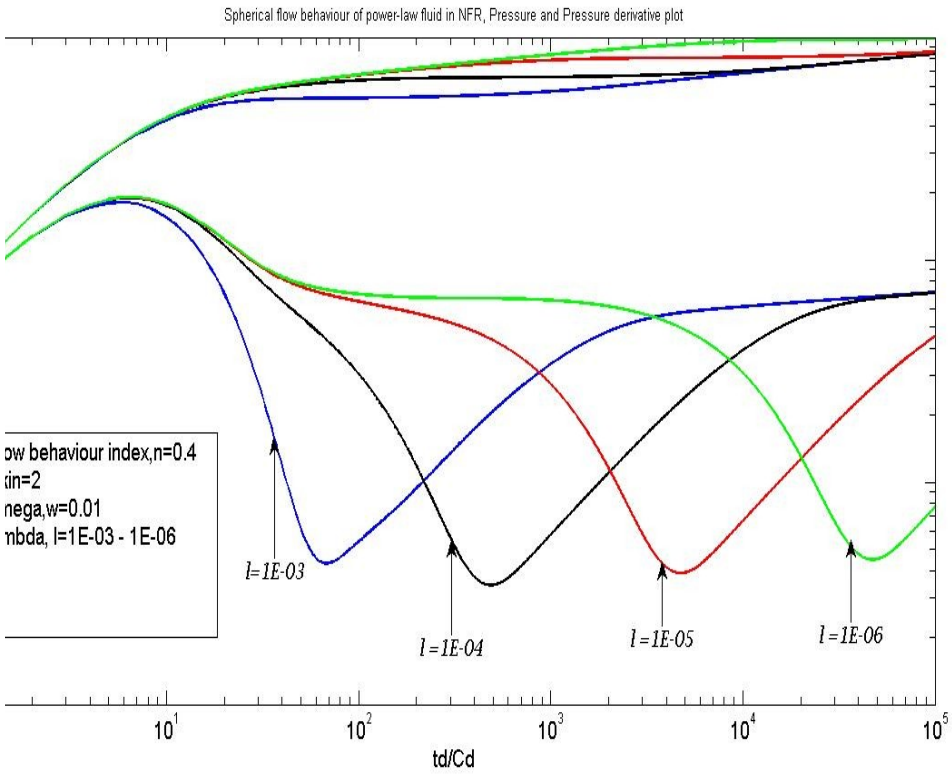

Fig.3.2.5 Pressure and Pressure derivative plot for Spherical flow behaviour of power-law fluid in NFR. (Skin=2; omega, ω= 1E-02; n=0.4)

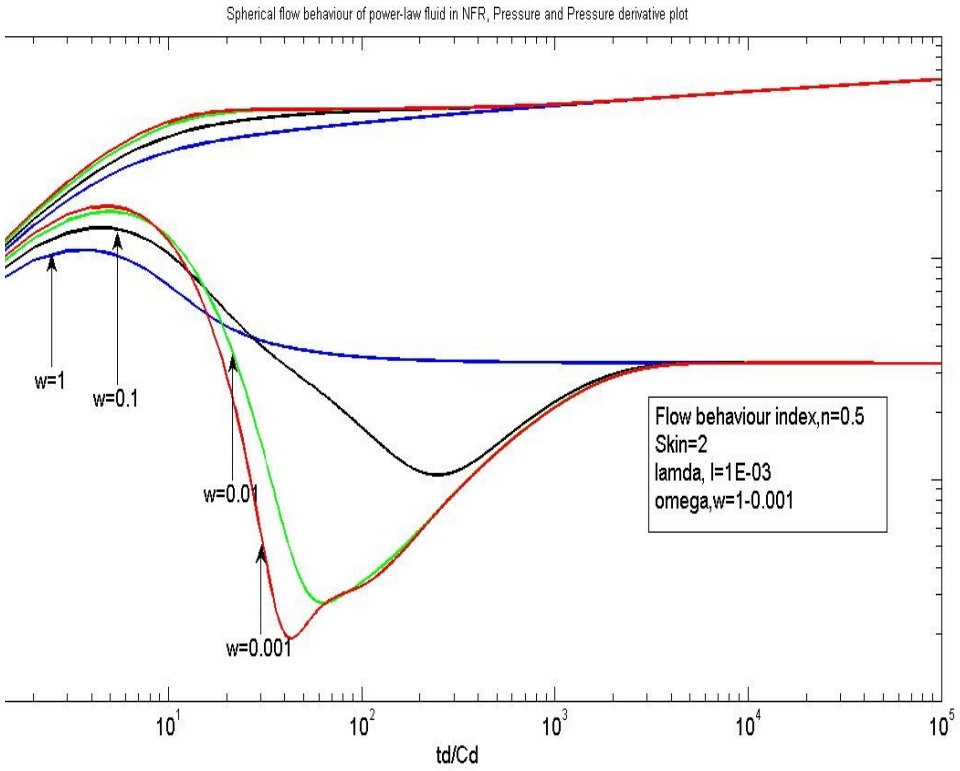

Fig.3.2.6 Pressure and Pressure derivative plot for Spherical flow behaviour of power-law fluid in NFR. (Skin=2; lambda, λ= 1E-03; n=0.5)

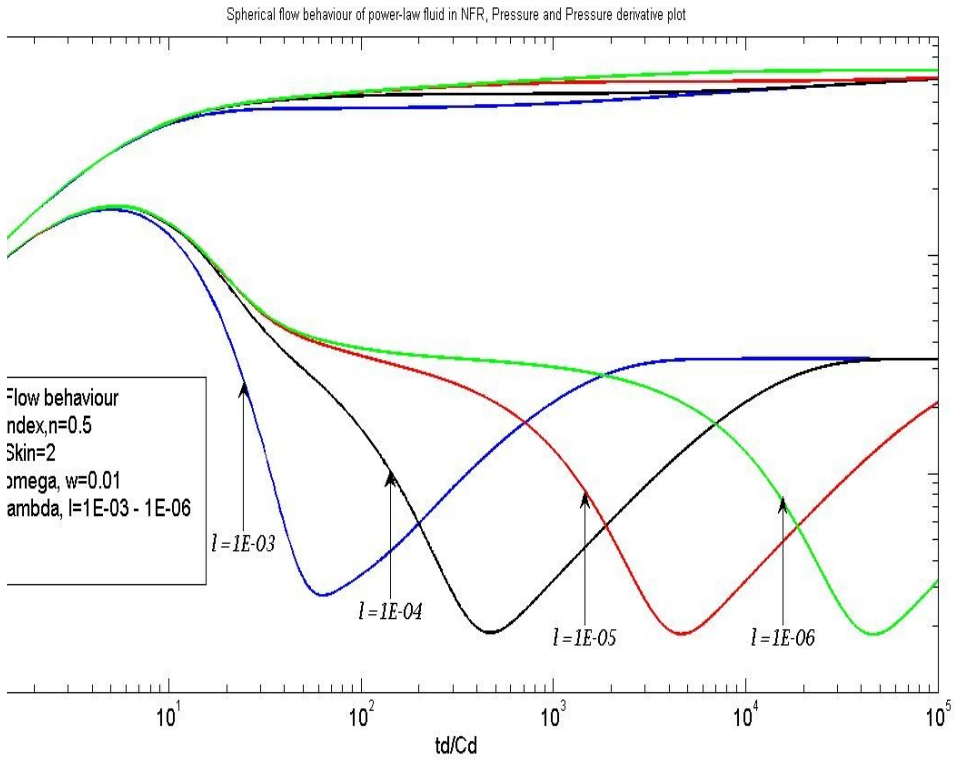

Fig.3.2.7 Pressure and Pressure derivative plot for Spherical flow behaviour of power-law fluid in NFR. (Skin=2; omega, ω= 1E-02; n=0.5)

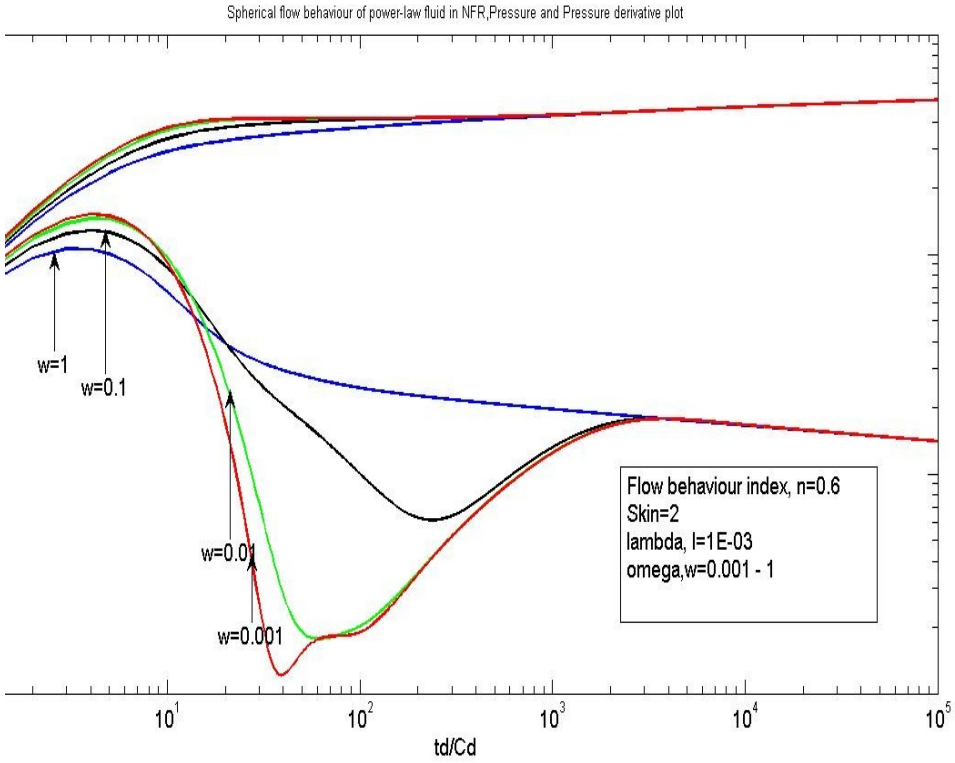

Fig.3.2.8 Pressure and Pressure derivative plot for spherical flow behaviour of power-law fluid in NFR. (Skin=2; lambda, λ= 1E-03; n=0.6)

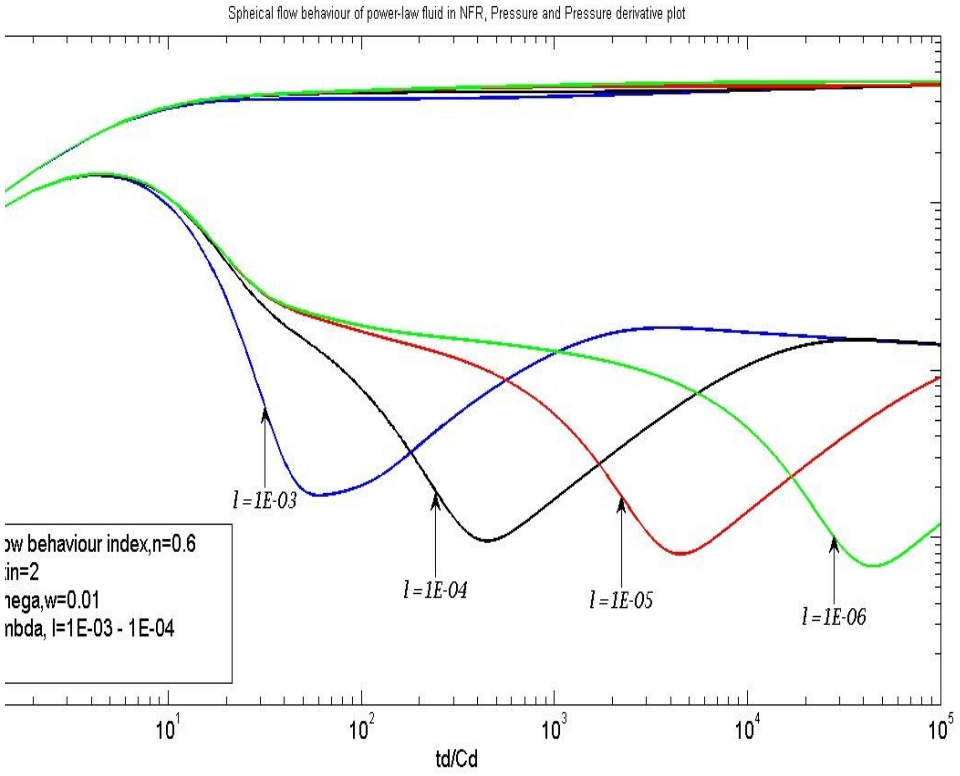

Fig.3.2.9 Pressure and Pressure derivative plot for Spherical flow behaviour of power-law fluid in NFR. (Skin=2; omega, ω= 1E-02; n=0.6)

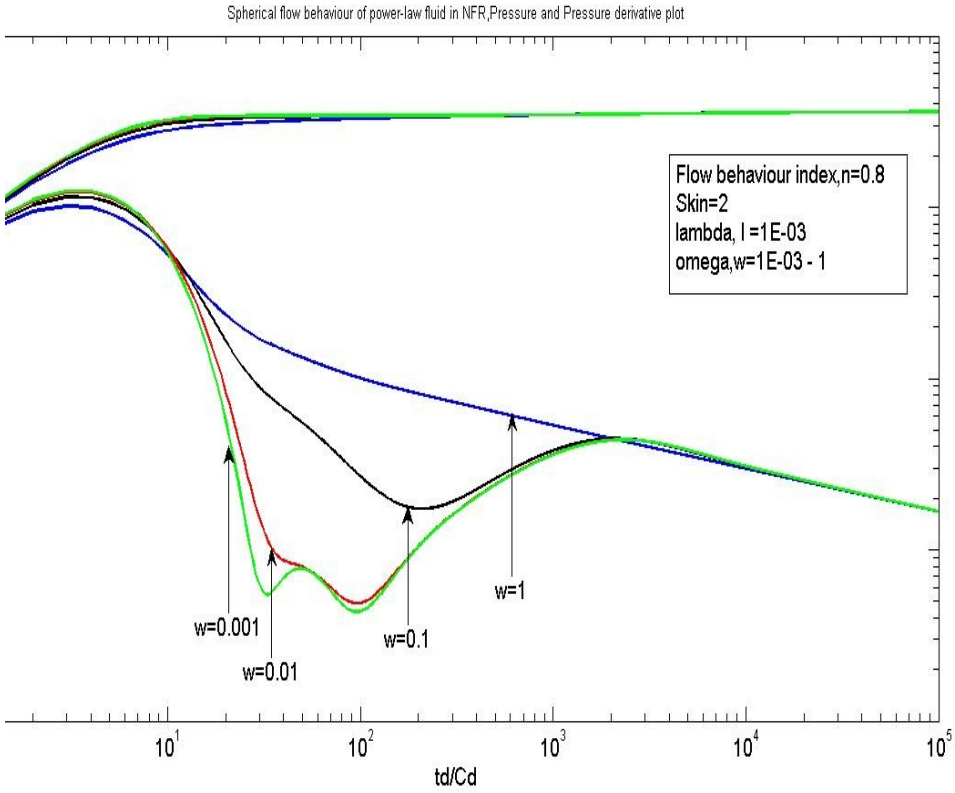

Fig.3.2.10 Pressure and Pressure derivative plot for Spherical flow behaviour of power-law fluid in NFR. (Skin=2; lambda, λ= 1E-03; n=0.8)

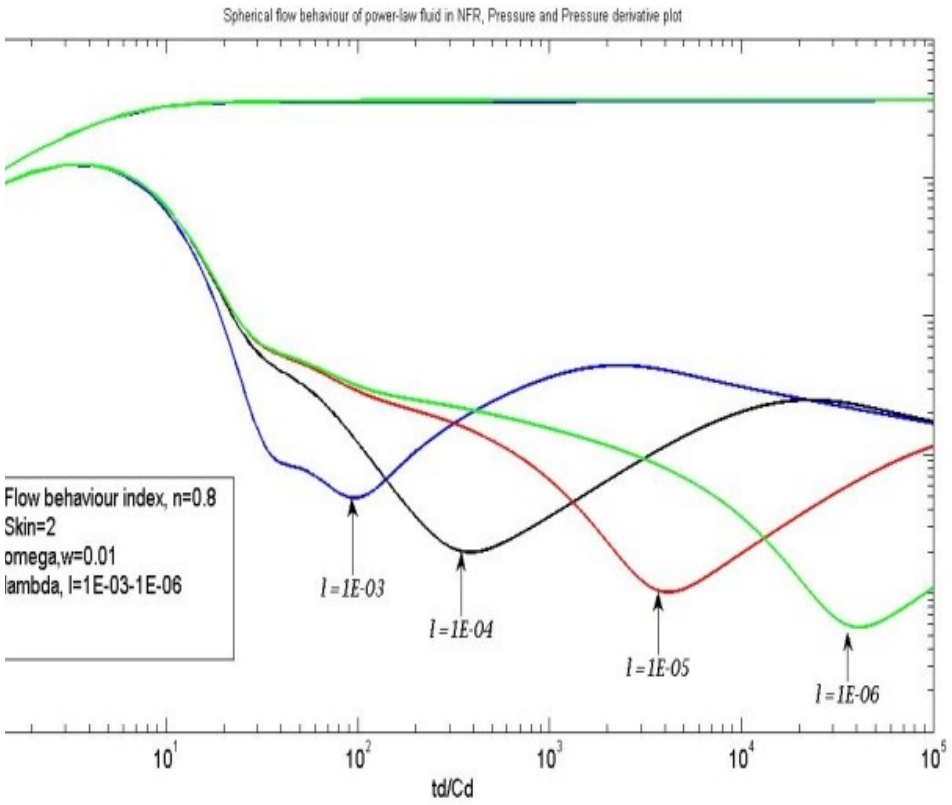

Fig.3.2.11 Pressure and Pressure derivative plot for Spherical flow behaviour of power-law fluid in NFR. (Skin=2; omega, ω= 1E-02; n=0.8)

3.3 Estimating Reservoir and Wellbore parameters

3.3.1 Tiab's Direct Synthesis Technique (TDS)

Similar to the established fluid mobility in Homogenous system, mobility in NFR is:

$$\frac{}{t)_{sp}}\left(\frac{t_{sp}}{(n\phi c_t)_f}\right)^{V}\left(\frac{2\pi}{q}\right)^{\frac{1+n}{2n-4}}\Bigg]^{\frac{1}{1-v}}$$

(54)

V is the slope of the Pressure derivative straight line;

Skin is given as:

$$\frac{k_f}{ff\cdot r_w^{1-2n}}\Bigg)\Bigg[(\Delta P_w)_{sp}-\frac{(\Delta P_w \times t)_{sp}}{V}\Bigg]+\frac{1}{1-2n}$$

(55)

And for the case n=0.5;

$$\frac{f(\Delta P_w)_{sp}}{\mu_{eff}}\Bigg]-0.3\ln\left[\left(\frac{2\pi}{q}\right)^{0.5}\frac{t_{sp}k_f}{0.5\phi c_t\mu_{eff}}\right]-0.54$$

(55a)

The two key parameters to characterize Naturally Fractured Reservoir, the Dimensionless storage coefficient (ω) and Inter-porosity flow parameter (λ) can be determined using Empirical correlation.

$$\Big]_{\min}$$

The plot of against Dimensionless storage coefficient (ω) at a constant value of λ, will give an empirical correlation for estimating ω. The Pressure derivative plots have shown that the value of (i.e. at the minimum inflection point of the derivative plot) for any λ value is approximately the same at a constant ω value. Dimensionless storage

coefficient ω, as it has been shown, is independent on time but the depth of the trough at the matrix-fracture transition flow region is dependent on the value of ω; the smaller the dimensionless storage coefficient ω, the deeper the trough, vice-versa.

Furthermore, the plot of against at a constant ω value will give an empirical correlation for estimating inter-porosity flow parameter (λ).

Figure (3.3.1) & (3.3.2) show the respective minimum Pressure derivative plot for different values of flow behaviour index, and their corresponding empirical correlations are outlined below:

Table 3.3.1 Empirical correlations for estimating ω and λ in dimensionless terms

irical correlation for ω	Empirical correlation for λ

Table 3.3.2 Empirical correlations for estimating ω and λ in real units

pirical correlation for ω	Empirical correlation for λ

$_{1}\Big)$

S_T = Total storativity of the formation:

Fig.3.3.1 Plot of minimum Dimensionless Pressure derivative against Dimensionless storage coefficient for n=0.2-0.8

Fig.3.3.2 Plot of minimum Dimensionless Pressure derivative against product of Dimensionless time and inter-porosity flow parameter for n=0.2-0.8.

Step by step procedure of using TDS technique in NFR assuming all characteristic points are observed

- Compute the pressure difference for Injection or Falloff test and the pressure derivative
- Plot on a log-log scale & versus injection time for Injection test or for Falloff test

- Identify the unit slope line at the early time of the plot representing the wellbore storage effect. Quantify the wellbore storage effect using equation (34)
- Identify the derivative straight line region (spherical flow region) on the plot and determine its slope V; from this obtain the flow behaviour index of the power-law fluid using

- Select any values of , and

in the spherical flow region of the plot; compute using

equation (54). Equation (24) can be used to estimate , thus

can be determined

- Identify the minimum pressure derivative coordinate at the matrix-fracture transition period and substitute these into the appropriate empirical correlation developed for estimating

and or obtain their estimate from figure (3.3.1) and (3.3.2) respectively.

$$= \left(\frac{2\pi}{q} \right)^{n} \frac{k_f}{\mu_{eff}} \frac{\left(\Delta P_w' \times t \right)_{\min}}{r_w^{1-2n}}$$

- Compute skin factor using equation (55) or (55a).

Chapter 4

Discussion and Conclusion

4.1 Application and Validation of Spherical flow Model of Power-law Fluid

Ershaghi et al. (1976) presented an example calculation for the application of pressure transient behaviour in Naturally Fractured Reservoir with spherical flow using pressure build-up test data. He was able to determine the fracture spherical permeability to be 49*md* by conventional method of well test analysis, and from Type curve match, dimensionless storage coefficient (ω) was determined to be 1. In this example, no skin damage around the wellbore was assumed.

Thus, the pressure build-up test data presented by Ershaghi et al. will be used for the validation of this work's pressure behaviour of power-law fluid flow in Naturally Fractured Reservoir. Below are the Reservoir and wellbore parameters and the pressure test data.

$(0.\ 122m)$

$= 1cp\ (10^{-3}\ pa.s)$

$(0.00368 m^3/s)$

Production time= 200*hrs*

h=70*ft* (21.336*m*)

$10^{-6}\ psi^{-1}$

$(1.26\times10^{-9} pa^{-1})$

To validate: Using Tiab's Direct Synthesis Technique

Step1: Computation of pressure and pressure derivative data

Table 4.1.1 Pressure and Pressure derivative data

t (*mins*)	t (*sec*)	Pws (*psi*)	dPws (*pa*)	t*dP'ws (*pa*)
0	0	2065		
0.093	5.58	2260	1344525	
0.186	11.16	2323	1778910	684817.643
0.373	22.38	2398	2296035	784342.142
0.467	28.02	2424	2475305	814357.789
0.654	39.24	2465	2758000	854591.746
0.934	56.04	2510	3068275	878773.463
1.869	112.14	2600	3688825	877575.956
2.803	168.18	2651	4040470	842323.952
4.67	280.2	2711	4454170	766252.809
9.34	560.4	2782	4943715	641408.634
18.69	1121.4	2840	5343625	502549.254
28.03	1681.8	2867	5529790	428850.479

37.38	2242.8	2884	5647005	387169.438
46.7	2802	2896	5729745	355170.499
56	3360	2905	5791800	331894.431
65	3900	2912	5840065	292835.918
74	4440	2917	5874540	267667.312
84.1	5046	2922	5909015	265885.142
93.4	5604	2926	5936595	255983.69
186	11160	2947	6081390	184075.127
280	16800	2957	6150340	126611.537
420	25200	2962	6184815	119422.42
514	30840	2966	6212395	243996.035
560	33600	2969.6	6237217	222913.049
654	39240	2971.9	6253076	

Step 2: Plot on a log-log scale pressure and pressure derivative data against time:

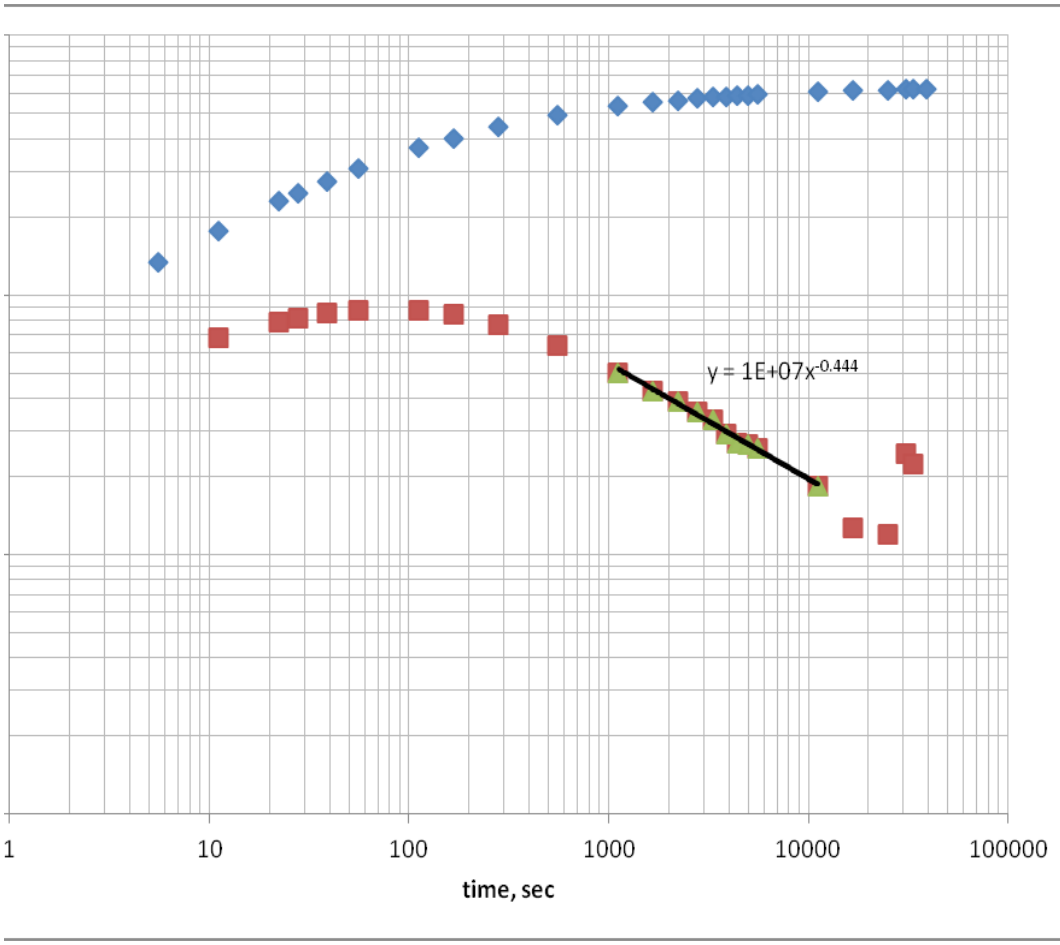

Fig.4.1.1 Pressure and Pressure derivative plot for a Pressure build-up test

Step 3: The early time unit slope line is not present in the plot above, therefore wellbore storage can be estimated using Type curve match point at early time straight line.

Step 4: The derivative straight line region (i.e. the spherical flow region) is as shown in the plot above and its slope is -0.444.

$$\frac{4)-1}{4)-2}$$

Thus, flow behaviour index ;

This implies the fluid flowing is a Newtonian fluid; hence, the power-law fluid model will be converted to Newtonian fluid model (by substituting n=1.0 and V= -0.5) for it to be applicable to the given example.

)065 pa 292835.92 pa

Step 5: ; ;

Using equation (54) which is derived from analytical solution, mobility is estimated below

$$\frac{}{5.92}\left(\frac{3900}{1.26\times10^{-9}}\right)^{-0.5}\left(\frac{2\pi}{0.00368}\right)^{-1}\Bigg]^{\frac{2}{3}}$$

$= 4.88\times10^{-11}\ m^2/pa.s$

Therefore,

$$\frac{^{11}\times1\times10^{-3}}{\times10^{-16}} = 49.5md$$

Step 6: Since this work is strictly on power-law fluid pressure behaviour, pressure and pressure derivative Type curve is not developed for Newtonian fluid pressure behaviour in NFR, hence the dimensionless storage coefficient and inter-porosity empirical correlation is not available for estimating these parameters in this example.

Step 7: Using equation (55) which is derived from analytical solution, the skin factor is estimated below

$$\left.\right)\times\frac{4.88\times10^{-11}}{0.122^{-1}}\Bigg]\left[5840065-\frac{292835.92}{0.5}\right]-\frac{1}{(1-(2\times1))}$$

= -0.93

From Type curve early time match point, wellbore storage can be estimated using equation (34) which is derived from type curve characteristic line.

)00 pa

;

$$\frac{21.336\times 3}{700000} = 3.12\times 10^{-6}\, m^3 \,/\, pa$$

A brief summary of results obtained from the above TDS analysis and the results obtained by Ershaghi et al. is shown below

Table 4.1.1 Reservoir and wellbore estimated properties

	This Study	Ershaghi et al.
Flow behaviour index, n	1.0	-
Spherical permeability, k_f	49.5*md*	49*md*
Skin, S	-0.93	0
Wellbore Storage, C	3.12E-6 m^3/pa	-
Storage coefficient, ω	-	1

The fracture spherical permeability obtained from the application of this study's model is in good agreement with that obtained through conventional well test analysis by Ershaghi et al. The skin factor estimated from TDS technique in this study gives a negative value close to the no wellbore damage assumption made in the reference analysis. The negative value obtained could only be interpreted to mean the wellbore is fractured. Since the well is not reported to be hydraulically fractured, deducing this example is that of pressure transient analysis in Naturally Fractured Reservoir will not be incorrect. This study also developed method for estimating wellbore storage as well as flow behaviour index value which were not provided in the reference analysis. Thus from the above close-match comparison, the model developed from this study for spherical flow pressure behaviour of power-law fluids in porous media is valid.

4.2 Discussion

The results of this work are presented as Type Curves and are discussed as follows:

1. As presented by Olanrewaju (1992) that lower pressure drop or pressure increase will be experienced in reservoir with non-Newtonian fluid flowing through its porous medium than for that of Newtonian fluid flow; the results of this study also shows that the lower the flow behaviour index value of power-law fluid the lower the pressure drop or the higher the pressure at the wellbore, vice versa.

2. The log-log plot of dimensionless pressure against dimensionless time (Fig.2.4.1) for a case without skin and storage effect in Homogenous reservoir system shows similar characteristic pressure behaviour as that presented by Ikoku et.al. (1978) for power-law fluids with radial flow assumption in porous media.

3. Late-time behaviour of the pressure derivative Type curve for Homogenous Reservoir system, as shown in Figure (2.4.2a), explains that pressure derivative straight line (i.e. at the spherical flow regime of the curve) gives a slope of -0.5 for a Newtonian fluid flow (n = 1), a positive slope for flow behaviour index less than 0.5 and a negative slope for flow behaviour index greater than 0.5; and for the case when n=0.5, the spherical flow behaviour is similar to radial flow behaviour of Newtonian fluid flow in porous media, but the former has dimensionless pressure derivative value of 0.3 at late-time. This is also shown in Figure (2.4.2b).

4. The pressure derivative Type Curve obtained for Homogenous Reservoir also shows that for large skin factor, there is a delay in the time it takes to reach the spherical flow period; likewise for high flow behaviour index value (say, n=1), it takes a longer time to reach stabilized late-time spherical flow regime (Fig 2.4.9 gives a clearer illustration of this).

5. The plot for spherical flow of power-law fluids in NFR shows three (3) characteristic flow regimes typical of NFR --- the early-time flow regime (which is dominated by wellbore storage, especially for the case with relatively large inter-porosity flow parameter), the matrix-fracture transition regime and the late-time flow regime. These plots, which are developed for different values of flow behaviour index, have exhibited the established norms in literature that the smaller the dimensionless storage coefficient the deeper the trough at the matrix-fracture transition period. It has also shown that the higher the flow behaviour index the deeper the trough regardless of dimensionless storage coefficient value.

6. Furthermore, the pressure derivative plot at late transition flow regime shows an approximate unit slope line for all values of flow behaviour index.

4.3 Conclusion

1. Pressure transient analysis for spherical flow behaviour of power-law fluids in Homogenous and Naturally Fracture Reservoir is studied and spherical flow models are developed using Type Curve matching and TDS.

2. New pressure and pressure derivative Type Curves are developed for different flow behaviour index of power-law fluid in Homogenous and NFR.

3. Analytical equations are developed for estimating reservoir, wellbore and power-law flow parameters in both Homogenous and NFR.

4. New empirical correlations are presented (for different values of flow behaviour index), for estimating the two key parameters to characterize Naturally Fractured Reservoir.

5. The new Type Curves and model presented are validated and can be used to analyze pressure transient behaviour in Polymer Injection/Fall-off well test in Homogenous and Naturally Fractured Reservoir.

6. The type curves developed for NFR in this study only incorporated a single value of skin, as the resulting number of plots would be much if it were to incorporate various skin values.

References

Bui, T. D. Mamora, D. D. Lee, W. J., Transient Pressure Analysis for Partially Penetrating Wells in Naturally Fractured Reservoir, SPE 60289, *Soc. Pet. Eng. J.,* 2000.

Engler, T., Interpretation of Pressure Tests in Naturally Fractured Reservoirs Without Type Curve Matching, *PhD Dissertation,* University of Oklahoma, 1995.

Ershaghi, I. Shie-Woo, R. and Hsun-Tiao, Y., Transient Data in Naturally Fractured Reservoir with Spherical flow, SPE 6018, *Soc. Pet. Eng. J.,* 1976.

Gidley, J. I., Holditch, A. S., Nierode, E. D., and Veatch, R. W., Recent Advances in Hydraulics Fracturing, *Soc. Pet. Eng. Monograph 12* (pg 179) (1989).

Herbert Harvey, A. and Menzie, D. E., Polymer Solution Flow in Porous Media, SPE 2369, *Soc. Pet. Eng. J.,* 1970.

Huh, C. and Snow, T. M., Well Test with a Non-Newtonian Fluid in the Reservoir, SPE 14453, *Soc. Pet. Eng. J.,* 1985.

Igbokoyi, A. O. and Tiab, D., New Type Curve for the Analysis of Pressure Transient Data Dominated by Skin and Wellbore Storage---Non-Newtonian Fluid, SPE 106997, *Soc. Pet. Eng. J.,* 2007.

Igbokoyi, A. O. and Tiab, D., A New Method of Well-test Analysis in Naturally Fractured Reservoir based on Elliptical Flow, SPE 116732, *Soc. Pet. Eng. J.,* 2008.

Ikoku, Chi U. and Ramey, H. J. Jr., Numerical Solution of the Non-linear Non-Newtonian Partial Differential Equation, SPE 7661, *Soc. Pet. Eng. J.,* 1978.

Ikoku, Chi U., Transient Flow of Non-Newtonian Power-law fluids in Porous Media, *PhD Dissertation,* Stanford University, Stanford, CA 1978.

Liu Ci-qun, Transient Spherical Flow of Non-Newtonian Power-law Fluids in Porous Media, *Applied Mathematics and Mechanics,* Vol.9, No.6, June 1988.

Odeh, A. S. and Yang, H. T., Flow of Non-Newtonian Power-law Fluids through Porous Media, SPE 7150, *Soc. Pet. Eng. J.,* 1979.

Okpobiri, G. A. and Ikoku, C. U., Pressure Transient Behaviour of Dilatant Non-Newtonian/Newtonian fluid Composite Reservoirs, SPE 12307, *Soc. Pet. Eng. J.,* 1983.

Olarewaju, J. S., A Reservoir Model of Non-Newtonian Fluid Flow, SPE 25301, *Soc. Pet. Eng. J.,* 1992.

Raghavan, R. and Clark, K. K., Vertical Permeability from Limited Entry Flow Tests in Thick Formations, SPE 4556, *Soc. Pet. Eng. J.,* 1975.

Sonatrach, K. S. Tiab, D. and Moncada, K., Pressure Transient Analysis of Partially Penetrating Wells in a Naturally Fractured Reservoir, SPE 104059, *Soc. Pet. Eng. J.,* 2006.

Van Pollen, H. K. and Jargon, J. R., Steady-state and Unsteady-state Flow of Non-Newtonian Fluids through Porous Media, SPE 1567, *Soc. Pet. Eng. J.,* 1969.

Vongvuthipornchai, S. and Raghavan, R., Well Test Analysis of Data Dominated by Storage and Skin: Non-Newtonian power-law fluids, SPE 14454, *Soc. Pet. Eng. J.,* 1987.

APPENDIX A – General

A –1 SI Metric Conversion Factors

$= Pa.s$

$1 = m$

$16 = m^2$

$00 = kPa$

$00 = m^3$

Table A –2: Pressure derivative for all n at $t_D/C_D = 1$

Flow behaviour index, n	
0.1	0.3925
0.2	0.3772
0.3	0.3621
0.4	0.3474
0.5	0.3333
0.6	0.3200
0.7	0.3076
0.8	0.2967
0.9	0.2879
1.0	0.2821

Pressure derivative weighted average is:

$$\underline{\quad_D / C_D)\big)} = 0.3117$$

A-2 Nomenclature

= Dimensionless pressure

= Initial reservoir pressure *psi, pa*

= Permeability *md,* m^2

= Formation thickness *ft, m*

= Flow rate *stb/d,* m^3/sec

= Effective viscosity *psi-hr-*ft^{1-n}*, pa-sec-*m^{1-n}

= Porosity fraction

= Consistency index

= Particle diameter *m*

= Total formation compressibility psi^{-1}, pa^{-1}

= Wellbore radius *ft, m*

= Spherical distance *ft, m*

= Dimensionless spherical distance

= Flow behaviour index

= Time *hr, sec*

= Dimensionless time

= Laplace variable

= Skin factor

= Superficial velocity in the spherical direction *ft/d, m/sec*

= Dimensionless wellbore storage coefficient

= Wellbore storage coefficient *bbl/psi, m^3/pa*

= Modified Bessel function first kind order V

= Gamma function

= Shape factor of the matrix block ft^2

= Euler's constant

= Inter-porosity flow parameter

= Dimensionless storage coefficient

APPENDIX B - Model Development Approach for Spherical flow pressure behaviour of power-law fluid in Porous media

B – 1 Homogenous Reservoir

Continuity equation of slightly compressible fluids for spherical flow in porous media, as presented by Liu Ci-qun, is:

$$\rho c_t \frac{\partial P}{\partial t}$$

(B-1-1)

But flow, V_r for non-Newtonian power-law fluids in porous media is:

(B-1-2)

Thus, the continuity equation for spherical flow of non-Newtonian power-law fluids is:

$$= n\phi c_t \frac{\partial P}{\partial t}$$

(B-1-3)

Substituting equation (B-1-2) into equation (B-1-3) and re-arranging

$$\frac{k}{\mu_{eff}}\frac{\partial P}{\partial r}\left)^{\frac{1}{n}}\right] = n\phi c_t \frac{\partial P}{\partial t}$$

$$\left.\right] = n\phi c_t \left(\frac{\mu_{eff}}{k}\right)^{\frac{1}{n}} \left(-\frac{\partial P}{\partial r}\right)^{\frac{n-1}{n}} \frac{\partial P}{\partial t}$$

(B-1-4)

Recall,

$$\frac{\mu_{eff}}{k}$$

(B-1-*)

Substituting (B-1-*) into RHS of equation (B-1-4)

$$\left.\right] = \left(\frac{n\phi c_t \mu_{eff}}{k}\right)\left(\frac{q}{2\pi}\right)^{n-1} r^{2(1-n)} \frac{\partial P}{\partial t}$$

(B-1-5)

To obtain the dimensionless definition of equation (B-1-5)

; &

Hence, the equation above becomes:

$$\frac{\partial P_D}{\partial r_D}\left.\right] = \left(\frac{n\phi c_t \mu_{eff}}{k}\right)\left(\frac{q}{2\pi}\right)^{n-1} \frac{r_w^{4-2n}}{t^*} r_D^{2(1-n)} \frac{\partial P_D}{\partial t_D}$$

$$\left(\frac{q}{2\pi}\right)^{n-1}$$

Substituting into the RHS of the above expression

$$\frac{\partial P_D}{\partial r_D}\right] = \frac{D r_w^{4-2n}}{t^*} r_D^{2(1-n)} \frac{\partial P_D}{\partial t_D}$$

Thus, $t^* = D r_w^{4-2n}$

From equation (B-1-*), ξ can be obtained as:

$$\frac{k}{\mu_{eff}}$$

ξ

(B-1-**)

Therefore equation (B-1-5) in its dimensionless form is:

$$\frac{\partial P_D}{\partial r_D}\right] = r_D^{2(1-n)} \frac{\partial P_D}{\partial t_D}$$

(B-1-6)

$$\frac{k}{r_w \mu_{eff}} (P_i - P)$$

Where,

(B-1-7)

(B-1-8)

(B-1-9)

$$r_w^2$$

(B-1-10)

The dimensionless initial and boundary conditions are:

(B-1-11)

(B-1-12)

$$\left(1 - C_D \frac{\partial P_{wD}}{\partial t_D}\right)$$

(B-1-13)

$$\frac{\partial P}{\partial t_D}\Big)_{r_D=1}$$

(B-1-14)

When equation (B-1-6) is linearized it becomes:

$$= r_D^{2(1-n)} \frac{\partial P_D}{\partial t_D}$$

(B-1-15)

Taking the Laplace of equation (B-1-15) gives:

$$- s\overline{P_D} r_D^{2(1-n)} = 0$$

(B-1-16)

Let

Equation (B-1-16) becomes:

$$_D \frac{\partial \overline{P_D}}{\partial r_D} - z\overline{P_D} r_D^{\ 2} = 0$$

(B-1-17)

Equation (B-1-17) is a modified spherical Bessel function; its solution is:

$$I_V\left(\alpha r_D{}^{2-n}\sqrt{s}\right)+B_2K_V\left(\alpha r_D{}^{2-n}\sqrt{s}\right)\Big]$$

(B-1-18)

Where and

Considering the boundary condition in equation (B-1-12); as ,

must remain bounded.

However ; to prevent $\rightarrow\infty$, $B_1=0$

Therefore equation (B-1-18) becomes:

$$_V\left(\alpha r_D{}^{2-n}\sqrt{s}\right)$$

(B-1-19)

Considering the Laplace transform of the inner boundary condition without wellbore storage and skin

$$\frac{1}{s}$$

(B-1-20)

Substituting equation (B-1-19) into (B-1-20) and taking the differential of the Bessel function and solving for B_2

$$\overline{\iota\sqrt{s}\right)}$$

;

Thus dimensionless pressure without wellbore storage and skin is given as:

$$\frac{\frac{1-2n}{2}K_V\left(\alpha r_D{}^{2-n}\sqrt{s}\right)}{s\sqrt{s}K_\beta\left(\alpha\sqrt{s}\right)}$$

Hence dimensionless wellbore pressure without skin and wellbore storage is:

$$\frac{K_V\left(\alpha\sqrt{s}\right)}{\sqrt{s}K_\beta\left(\alpha\sqrt{s}\right)}$$

(B-1-21)

Recall, dimensionless wellbore pressure in Laplacian space with skin and storage is expressed as:

$$\frac{s\overline{P_{wD*}}+S}{sC_D\left(sP_{wD*}+S\right)\Big]}$$

(B-1-22)

Substituting equation (B-1-21) into (B-1-22)

$$\frac{K_V\left(\alpha\sqrt{s}\right)+S\sqrt{s}K_\beta\left(\alpha\sqrt{s}\right)}{K_\beta\left(\alpha\sqrt{s}\right)+sC_D\left[K_V\left(\alpha\sqrt{s}\right)+S\sqrt{s}K_\beta\left(\alpha\sqrt{s}\right)\right]\Big]}$$

(B-1-23)

For Newtonian fluid (i.e. n=1) spherical flow behaviour, equation (B-1-23) becomes:

$$\frac{K_{\frac{1}{2}}\left(\alpha\sqrt{s}\right)+S\sqrt{s}K_{\frac{3}{2}}\left(\alpha\sqrt{s}\right)}{K_{\frac{3}{2}}\left(\alpha\sqrt{s}\right)+sC_D\left[K_{\frac{1}{2}}\left(\alpha\sqrt{s}\right)+S\sqrt{s}K_{\frac{3}{2}}\left(\alpha\sqrt{s}\right)\right]\Big]}$$

(B-1-24)

For the case where S≠0 and C_D=0, equation (23) reduces to:

$$\frac{\left(\alpha\sqrt{s}\right)}{\sqrt{s}K_\beta\left(\alpha\sqrt{s}\right)}+\frac{S}{s}$$

(B-1-25)

Liu Ci-qun presented an analytical Laplace inversion of equation (B-1-25) without skin (i.e. S=0) as:

$$\frac{-2n)^{2V} t_D{}^{V}}{2n)\Gamma\left(\frac{3}{4-2n}\right)} - \frac{1}{1-2n}$$

(B-1-26)

Thus for the case with skin, equation (B-1-25) becomes:

$$\frac{-2n)^{2V} t_D{}^{V}}{2n)\Gamma\left(\frac{3}{4-2n}\right)} - \frac{1}{1-2n} + S$$

(B-1-27)

The solution above is the analytical solution for the long-time approximation for all flow behaviour index except for n=0.5, in which the above equation is not valid. Therefore the solution for case when n=0.5 goes thus:

Recall, equation (B-1-25),

$$\frac{\left(\frac{2}{3}\sqrt{s}\right)}{\Gamma\left(\frac{2}{3}\sqrt{s}\right)} + \frac{S}{s}$$

For n=0.5,

(B-1-27a)

For early time behaviour of P^D, the limit of dimensionless pressure in Laplace space as s tends to infinity is taken. But,

$$\sqrt{\left(\frac{3\pi}{4\sqrt{s}}\right)} e^{-\frac{2}{3}\sqrt{s}}$$

(B-1-27b)

$$\sqrt{\left(\frac{3\pi}{4\sqrt{s}}\right)} e^{-\frac{2}{3}\sqrt{s}}$$

(B-1-27c)

So at early time, substituting equations (B-1-27b) and (B-1-27c) into equation (B-1-27a), we have:

(B-1-27d)

Taking the inverse Laplace of equation (B-1-27d)

(B-1-27e)

Equation (B-1-27e) gives the early time solution for power-law fluid (when n=0.5) in Homogenous reservoir with spherical flow.

The late-time solution for the above power-law fluid case goes thus:

For late-time behaviour of dimensionless pressure, the limit of as s tends to zero is taken.

$$\ln\left(\frac{s}{2}\right)+\gamma$$

(B-1-27f)

And for small argument

$$\left(\frac{1}{2}s\right)^{-V}$$

$$=\frac{3}{2\sqrt{s}}$$

Thus,
(B-1-27g)

Substituting equation (B-1-27f) and (B-1-27g) into (B-1-27a)

$$\frac{n\sqrt{s}-\ln 3+\gamma}{s}\Bigg]+\frac{S}{s}$$

(B-1-27h)

Taking the inverse Laplace of equation (B-1-27h)

$$\frac{\gamma}{3}+\frac{2\ln 3}{3}+S$$

(B-1-27i)

Thus, equation (B-1-27i) gives the late time solution for power-law fluid (when n=0.5) in Homogenous reservoir with spherical flow.

B - 2 Naturally Fractured Reservoir

The continuity equation for spherical flow of non-Newtonian power-law fluid in porous media is given as:

$$\frac{k}{\mu_{eff}}\frac{\partial P}{\partial r}\left[\frac{\partial P}{\partial r}\right]^{\frac{1}{n}}=n\phi c_t\frac{\partial P}{\partial t}$$

(B-2-1)

From the above equation, the continuity equation for power-law fluid flow through the fracture in NFR can be written as:

$$\frac{k_f}{\mu_{eff}}\frac{\partial P_f}{\partial r}\left[\frac{\partial P_f}{\partial r}\right]^{\frac{1}{n}}=n[\phi c_t]_f\frac{\partial P_f}{\partial t}-q$$

(B-2-2)

And for flow in matrix we have:

$$\frac{k_m}{\mu_{eff}}\frac{\partial P_m}{\partial r}\Big)^{\frac{1}{n}}\Big] = n[\phi c_t]_m \frac{\partial P_m}{\partial t} + q$$

(B-2-3)

Assuming pseudo-steady state flow from matrix to fracture

$$\frac{P_m}{)t}$$

(B-2-4)

Substituting equation (B-2-4) into (B-2-2):

$$\frac{P_f}{)r}\Big] = \Big(\frac{n\mu_{eff}}{k_f}\Big)\Big(\frac{q}{2\pi r^2}\Big)^{n-1}\Big[[\phi c_t]_f \frac{\partial P_f}{\partial t} + [\phi c_t]_m\Big]$$

(B-2-5)

The dimensionless definition of equation (B-2-5) is:

$$\frac{\partial P_{fD}}{\partial r_D}\Big] = r_D{}^{2(1-n)}\Big[\omega\frac{\partial P_{fD}}{\partial t_D} + (1-\omega)\frac{\partial P_{mD}}{\partial t_D}\Big]$$

(B-2-6)

Where,

$$\frac{k_j}{\mu_{eff} r_w}\big(P_i - P_j\big)$$

(B-2-7)

Subscript j = f or m, the indices for fracture (f) and (m)

$$\frac{q}{2\pi}\Big)^{n-1}\big([\phi c_t]_f + [\phi c_t]_m\big)$$

;

(B-2-8)

;

(B-2-9)

Warren and Root presented Matrix-Fracture interface condition as:

$$P_f \Big)$$

(B-2-10)

Equating equation (B-2-10) to (B-2-4) we have:

$$= \frac{\Omega k_m}{\mu_{eff}} \Big(P_m - P_f \Big)$$

(B-2-11)

The dimensionless form of equation (B-2-11) is:

$$P_{fD} - P_{mD} \Big)$$

(B-2-12)

Where,

$$\frac{q}{\pi r_w^{\,2}} \Big)^{n-1} \div \Big)$$

;

(B-2-13)

Taking the Laplace transform of equation (B-2-6) and (B-2-12) we obtain:

$$\frac{\overline{P_{fD}}}{r_D} \Big) \Big] = r_D^{\,2(1-n)} \Big[\omega s \overline{P_{fD}} + (1-\omega) s \overline{P_{mD}} \Big]$$

(B-2-14)

$$\overline{P_{fD}} - \overline{P_{mD}} \Big)$$

(B-2-15)

Re-arranging equation (B-2-15) and substituting into (B-2-14) diffusivity equation for NFR is:

$$\frac{)\overline{P_{fD}}}{\partial r_D}\Bigg] = r_D{}^{2(1-n)} sf(s)\overline{P_{fD}}$$

(B-2-16)

$$\frac{)s+\lambda}{)+\lambda}$$

Following the general procedure for applying Homogenous solution to Double porosity system, the Laplacian space solution of spherical flow behaviour of power-law fluid in NFR can be written as:

$$\frac{\cdot_V\left(\alpha\sqrt{sf(s)}\right)}{\overline{(s)}K_\beta\left(\alpha\sqrt{sf(s)}\right)}$$

(B-2-17)

Incorporating skin and wellbore storage effect, the above equation turns:

$$\frac{K_V\left(\alpha\sqrt{sf(s)}\right)+S\sqrt{sf(s)}K_\beta\left(\alpha\sqrt{sf(s)}\right)}{\overline{(s)}K_\beta\left(\alpha\sqrt{sf(s)}\right)+sC_D\left\{\left(K_V\left(\alpha\sqrt{sf(s)}\right)+S\sqrt{sf(s)}K_\beta\left(\alpha\sqrt{sf(s)}\right)\right)\right\}\Bigg]}$$

(B-2-18)

To develop the solution of the above equations, for purpose of interpretation, the Laplace inversion of equation (B-2-17) will be done analytically while (B-2-18) will be done numerically.

The approximate series expansion of equation (B-2-17) is:

$$\frac{\left(\frac{\cdot}{\cdot}\right)^u}{\overline{f(s)}}\left[1-\frac{y}{Vx}\left(\frac{R}{2}\right)^{2V}+\frac{x}{\beta y}\left(\frac{R}{2}\right)^{2\beta}+....\right]$$

(B-2-19)

Where,

;

;

;

;

$$\frac{)s+\lambda}{)+\lambda}$$

Recall, and for early time solution,

, since is a very small number

Therefore early time solution of equation (B-2-19), considering the first two terms, is:

$$\left[\frac{x\left(\frac{R}{2}\right)^{u}}{y}-\frac{1}{V}\left(\frac{R}{2}\right)^{2V+u}\right]$$

(B-2-20)

Substituting for x, y, u, V, R and

$$\frac{\left(\frac{-2n}{-2n}\right)}{\left(\frac{3}{-2n}\right)}\omega^{\frac{2n-1}{4-2n}}s^{\frac{4n-5}{4-2n}}-\frac{1}{(1-2n)s}$$

(B-2-21)

Taking inverse Laplace of the above equation

$$\frac{2n)^{\frac{2-4n}{4-2n}}}{\left(\frac{3}{4-2n}\right)}\left(\frac{t_D}{\omega}\right)^{\frac{1-2n}{4-2n}}-\frac{1}{1-2n}$$

(B-2-22)

Thus the early time solution with skin factor incorporated is:

$$\frac{2n)^{2V}}{\neg\left(\frac{3}{4-2n}\right)}\left(\frac{t_D}{\omega}\right)^{V}-\frac{1}{1-2n}+S$$

(B-2-23)

For Late-time solution ; hence, following the above steps, the Late-time solution is:

$$\frac{\cdot 2n)^{2V}}{\Gamma\left(\frac{3}{4-2n}\right)}t_D{}^{V}-\frac{1}{1-2n}+S$$

(B-2-23a)

Equations (B-2-23) and (B-2-23a) above for pressure behaviour of power-law fluid in NFR with spherical flow, is valid for all flow behaviour index except for n=0.5 which has its special solution; its solution is given below:

Recall equation (B-2-17),

$$\frac{\left(\frac{2}{3}\sqrt{s}\right)}{\left(\frac{2}{3}\sqrt{s}\right)}+\frac{S}{s}$$

For n=0.5,

(B-2-23b)

And for early time solution,

, thus:

$$\frac{\left(\frac{2}{3}\sqrt{s\omega}\right)}{K_1\left(\frac{2}{3}\sqrt{s\omega}\right)}$$

(B-2-23c)

Also for early time behaviour of P_{wD}, the limit of as s tend to infinity is taken

But,

$$\sqrt{\frac{3\pi}{4\sqrt{s\omega}}}e^{\frac{-2}{3}\sqrt{s\omega}}$$

(B-2-23d)

And

$$\sqrt{\frac{3\pi}{4\sqrt{s\omega}}}e^{\frac{-2}{3}\sqrt{s\omega}}$$

(B-2-23e)

Therefore, substituting equation (B-2-23d) & (B-2-23e) into equation (B-2-23):

(B - 2- 23f)

Taking inverse Laplace of equation (B-2-23f)

(B- 2- 23g)

Equation (B-2-23g) gives the early time solution for power-law fluid (when n=0.5) in NFR with spherical flow behaviour.

The late time solution for power-law fluid (when n=0.5) in NFR with spherical flow is:

$$\frac{\gamma}{3}+\frac{2\ln 3}{3}$$

(B- 2- 23h)